The Astrophysical Journal, 583:632–648, 2003 February 1

THE UNIFIED MODEL AND EVOLUTION OF ACTIVE GALAXIES: IMPLICATIONS FROM A SPECTROPOLARIMETRIC STUDY

Hien D. Tran
Department of Physics and Astronomy, Johns Hopkins University, Baltimore, MD 21218; tran@pha.jhu.edu
Received 2002 August 14; accepted 2002 October 9

ABSTRACT

We extend the analysis presented in Paper I of a spectropolarimetric survey of the CfA and 12 μm samples of Seyfert 2 galaxies (S2s). We confirm that polarized (hidden) broad-line region (HBLR) S2s tend to have hotter circumnuclear dust temperatures, show mid-IR spectra more characteristic of Seyfert 1 galaxies (S1s), and are intrinsically more luminous than non-HBLR S2s. The levels of obscuration and circumnuclear star formation, however, appear to be similar between HBLR and non-HBLR S2 galaxies, based on an examination of various observational indicators. HBLR S2s, on average, share many similar large-scale, presumably isotropic, characteristics with S1s, as would be expected if the unified model is correct, while non-HBLR S2s generally do not. The active nuclear engines of non-HBLR S2s, then, appear to be truly weaker than HBLR S2s, which in turn are fully consistent with being S1s viewed from another direction. There is also evidence that the fraction of detected HBLRs increases with the radio power of the active galactic nucleus. Thus, all S2 galaxies may not be intrinsically similar in nature, and we speculate that evolutionary processes may be at work.

Subject headings: galaxies: active — galaxies: Seyfert — polarization

On-line material: color figures

1. INTRODUCTION

The discovery nearly two decades ago of polarized broad permitted emission lines in NGC 1068 (Miller & Antonucci 1983; Antonucci & Miller 1985) demonstrated that some Seyfert 2 galaxies (S2s) were basically the same type of object as Seyfert 1 galaxies (S1s) but viewed from a different direction. Since then, there have been plenty of other examples of polarized (hidden) broad-line regions seen in reflected light (HBLRs) in nearly all types of active galactic nuclei (AGNs), ranging from the lowly LINERs (Barth, Filippenko, & Moran 1999), to Seyferts (Miller & Goodrich 1990; Tran, Miller, & Kay 1992a; Tran 1995, 2001; Young et al. 1996b; Heisler, Lumsden, & Bailey 1997; Moran et al. 2000; Lumsden et al. 2001), to ultraluminous infrared galaxies (ULIRGs; Hines et al. 1995, 1999; Goodrich et al. 1996; Tran et al. 1999; Tran, Cohen, & Villar-Martin 2000), to powerful radio galaxies near and far (e.g., Antonucci 1984; Tran, Cohen, & Goodrich 1995; Cimatti & di Serego Alighieri 1995; Young et al. 1996a; Ogle et al. 1997; Tran et al. 1998; Cohen et al. 1999). This orientation-based unification model (UM; Antonucci 1993) may even be applicable to the luminous broad absorption line quasars (BAL QSOs; Cohen et al. 1995; Goodrich & Miller 1995; Hines & Wills 1995).

Although the UM is widely accepted for many classes of AGNs, especially Seyfert galaxies, where there are many fine examples, there is still no consensus on its general applicability for *all* members of each class. In fact, a number of studies have reported some disturbing differences between S1s and S2s that appear to be inconsistent with the simple orientation-based UM. These include suggestions that S2s tend to reside in hosts with enhanced star-forming activity (Maiolino et al. 1995; Gu, Huang, & Ji 1998), with a higher frequency of companions (de Robertis, Yee, & Hayhoe 1998; Dultzin-Hacyan et al. 1999), or richer in dust features (Malkan, Gorjian, & Tam 1998, hereafter MGT98) compared to S1s. Recently, Tran (2001, hereafter Paper I) presented the results of a large spectropolarimetric survey of S2s from the CfA (Huchra & Burg 1992) and 12 μm (Rush, Malkan, & Spinoglio 1993) samples. The main conclusion from this paper is that there appears to be a class of S2 galaxies that are intrinsically weak and, as far as can be determined, lack (or possess very weak) broad-line regions (BLRs) that characterize the genuine hidden S1 galaxies. This class of "real" S2s represents approximately half of the total currently known S2 population.[1] In this paper, we extend the analysis of the data from the survey of Paper I, compare them with S1s, and present some additional evidence for the idea of two different types of S2s and its implications. We assume $H_0 = 75$ km s^{-1} Mpc^{-1}, $q_0 = 0$, and $\Lambda = 0$ throughout this paper.

2. DATA AND RESULTS

The spectropolarimetric observations of the CfA and 12 μm S2s are briefly described in Paper I. All of the observations were made at Lick and Palomar Observatories, except one (for F08572+3915) that was obtained at Keck Observatory. These observations were made with the main goal of searching for polarized broad Hα, which is the strongest of the hydrogen Balmer lines. Accordingly, they were optimized for the red spectral region, around the wavelength of redshifted Hα. Observations at Lick were made with the 3 m Shane telescope and the Kast double spectrograph

[1] Note that the use of "pure" S2s in Paper I and in Cid Fernandes et al. (2001) refers to different types of Seyfert 2 galaxies. Cid Fernandes et al. used "pure" S2s to refer to those without a dominant contribution from a starburst component but not necessarily without HBLRs. In Paper I, we used the term "pure" S2s to refer to non-HBLR S2s regardless of the starburst contribution. To avoid confusion, whenever possible we use "real" S2s to refer to non-HBLR S2s in this paper.

(Miller & Stone 1993), using a dichroic that splits the light at 4600 Å. A 600 groove mm^{-1} grating was used on the red side, while a 600 groove mm^{-1} grism was used on the blue side, providing a resolution of $\sim$6 Å for both sides. The wavelength coverage was typically 3200–4500 Å in the blue and 4600–7400 Å in the red, both on 400 pixel × 1200 pixel CCDs. At Palomar, spectropolarimetry was obtained with the double spectrograph (Oke & Gunn 1982) on the 5 m Hale telescope. In combination with a 5500 Å dichroic, we used a 300 groove mm^{-1} grating on the blue and a 316 groove mm^{-1} grating on the red, giving a typical wavelength coverage of 3600–5500 and 5500–8000 Å, respectively, with 800 pixel × 800 pixel CCDs. The spectral resolution was about 6 Å in the red and 8 Å in the blue. The single observation at Keck was made on 1994 October 29 (UT) with the polarimeter module installed on the Low Resolution Imaging Spectrometer (Oke et al. 1995) at the 10 m Keck I telescope. A 300 groove mm^{-1} grating was used with a 2048 × 2048 CCD detector to give a wavelength coverage of 3900–8900 Å and a resolution of $\sim$10 Å. For all observations, we employed a long slit with width ranging from 1″ (Keck) to 2″ (Palomar) or 2″.4 (Lick), centered on the nucleus and oriented mostly east-west and, in some cases, near the parallactic angle. Data were reduced using the standard VISTA procedures used in previous studies (see, e.g., Tran 1995).

As in Paper I, we refer to galaxies classified as H II, LINER, or starburst galaxies as the " HLS " sample. There are 16 such sources, and they are listed in Table 1. We display these galaxies in figures but have excluded them from all statistical analyses in this paper for Seyfert galaxies. The total number of S2s in the 12 μm sample is 51, of which 43 have been observed by either this or other studies. Excluding the intermediate Seyferts (i.e., S1.8, S1.9), all 14 CfA galaxies classified as S2 by Osterbrock & Martel (1993, hereafter OM93) have been observed spectropolarimetrically. Most of the remaining eight unobserved S2s are unreachable by telescopes employed in the survey. The main disadvantage of the 12 μm sample is that its spectroscopic classification is much poorer than that of the CfA sample, which has been further refined by OM93. In fact, the classification of Rush et al. (1993) was found to contain many misclassifications. In our study, we take advantage of the high signal-to-noise ratio (S/N) spectra as a by-product of the spectropolarimetric observations and reclassify these objects.

The main result of the survey, the presence or absence of HBLR detection for our sample galaxies, is presented in Table 1, along with their most relevant X-ray, optical, IR, and radio properties. References are given for the sources of the data, most of which have been collected from the literature. The optical data, such as the [O III] flux and Balmer decrement, when not previously available, have been measured directly from our spectroscopy. We note that only one galaxy (F08572+3915), which belongs in the HLS class, was observed at Keck. Although the S/N is superb for this object, it does not show an HBLR. All other sources were observed at Lick or Palomar Observatory. Thus, to a good approximation, the detections of HBLRs in the sample S2s are probed to similar depths. Results from the following surveys have also been used: Miller & Goodrich (1990), Tran et al. (1992a), Young et al. (1996b), Heisler et al. (1997a), Barth et al. (1999), Moran et al. (2000), and Lumsden et al. (2001). The literature data for S1s for the combined CfA and 12 μm sample are shown in Table 2. We have revised the original S1 table of Rush et al. (1993) to include only S1 and S1.5 galaxies, excluding those classified as S1.8 or S1.9. In order to avoid biases, we have also removed several highly radio-luminous 3C galaxies from their S1 list, as noted in the table.

2.1. *Discrepancy in HBLR S2 Fraction between the CfA and 12 μm Samples?*

In Paper I, it was noted that the detection rate of HBLRs is significantly lower in the CfA sample ($4/14 = 29\%$) than in the 12 μm sample ($21/43 = 49\%$), although the CfA detection rate is similar to that reported by previous studies (e.g., Moran et al. 2000). Because the 12 μm sample selects objects in the IR and therefore is well suited for picking up galaxies that are dust obscured, it was suggested that the $\approx$50% HBLR detection rate may be more representative than the lower 30%–35% suggested by the CfA sample and other optically defined samples. The optically selected CfA sample, on the other hand, while avoiding the normal biases suffered by the traditional UV-access searches by spectroscopically identifying a magnitude-limited sample of nearby galaxies, may have missed the more dust obscured AGNs.

Note that in surveying the CfA sample, we chose to observe only those classified as strict S2s by OM93. Seyfert 1.8s and 1.9s were intentionally excluded. This was not done for the 12 μm sample, mainly because no such detailed classification was available for it. Could this have been the source of the discrepancy in the detection rate? This is unlikely to be the case. Goodrich (1989) carried out a spectropolarimetric survey of Seyfert 1.8s and 1.9s and found that only three out of 12 such galaxies showed polarization, indicating that their broad lines were due to scattered light. If we assume a similar detection rate for the S1.8s and S1.9s in the CfA sample,[2] this suggests that not including them in the survey cannot explain this discrepancy.

Recently, Moran et al. (2001) reported that two of the CfA S2s identified as non-HBLR in Paper I (NGC 5347 and NGC 5929)[3] were found to show weak polarized broad lines in the more sensitive Keck observations. If confirmed, it would bring the HBLR S2 fraction in the CfA to 43%, more consistent with that reported for the 12 μm sample. Thus, there may not be a discrepancy in the HBLR S2 fraction between the two samples, and 50% remains a good representative value for the fraction of the total S2 population that contains powerful hidden S1 nuclei. However, to avoid mixing surveys with different detection limits and to remain consistent with our original detection limit of 3–5 m class telescopes, in the rest of the analysis in this paper we opt to keep these two objects in the non-HBLR sample. The difference caused by moving them to the HBLR classification is small and does not significantly alter the main conclusions of this paper.

Since non-HBLR S2s are shown to be systematically weaker than their HBLR counterparts (this work; Paper I; Lumsden & Alexander 2001), it is possible that with deeper observations some of the non-HBLR S2s reported in this

[2] Incidentally, two of the objects surveyed by Goodrich (1989) are in the CfA sample (Mrk 744 and Mrk 471), both of which turned out to show little or no polarization.

[3] NGC 5929 was also reported as a non-HBLR S2 by Lumsden et al. (2001).

TABLE 1

HBLR and Non-HBLR Seyfert 2 Galaxies of the CfA and 12 μm Samples

Name	Other ID	z	$f_{[O III]}$	[O III]/Hβ	Hα/Hβ	f_{25}	f_{60}	f_{100}	$S_{20 cm}$	HX	N_H	EW(Fe)	Reference
HBLR Seyfert 2 Galaxies													
F00521−7054		0.06890	0.0052	1.00	5.77	0.90	0.92	0.40	17.5[a]	<3.18	...		1/2
F01475−0740		0.01767	0.0053	0.73	7.62	0.84	1.10	1.05	318.8	...	...		3P, 4/
F02581−1136	MCG −2-8-39	0.02998	0.0014	1.28	5.13	0.46	0.54	0.85	9.0	...	...		3L, 5/
F04385−0828		0.01510	0.00035	0.78	9.2	1.70	2.91	3.55	17.4	0.60	...		3LP, 6/2
F05189−2524		0.04256	0.00028	1.05	23.4	3.41	13.27	11.90	28.7	0.61	643.	130	1, 7, 8/9, 10
F15480−0344		0.0300	0.018	1.16	5.99	0.72	1.09	4.05	42.2	...	...		3P, 1, 6, 11, 12/
F22017+0319		0.06110	0.0179	0.99	4.0	0.59	1.31	1.65	18.3	0.36	5000		3P, 1/13
IC 5063		0.01135	0.093	1.01	5.80	3.95	5.79	3.66	1260	3.0	2400.	80	14, 15, 9/9
MCG −3-34-64	PKS B1319−164	0.01718	0.160	1.06	4.17	2.88	6.22	6.37	251.8	0.65	7600	200	1, 16, 9/9
Mrk 348	NGC 262	0.01514	0.042	1.08	6.02	1.02	1.43	1.43	281.5	2.21	1060.	230	17, 18/9
MCG −3-58-7	F22469−1932	0.03174	0.0251	1.14	5.5	0.98	2.60	3.62	12.7	...	...		3P/
Mrk 463 E		0.05100	0.073	0.86	5.59	1.49	2.21	1.87	376.0	0.09	1600.	<670	17, 18/9
NGC 1068[b]		0.00379	2.05	1.08	7.00	92.7	198.0	259.77	4845	0.35	100000	1210	19, 18, 15/9
NGC 424	Tol 0109−383	0.01166	0.042	0.755	5.16	1.76	2.00	1.74	23.3	0.12	10000	1600	20, 21/22
NGC 4388[b]		0.00842	0.048	1.10	5.50	3.72	10.46	18.10	118.5	4.30	4200.	732	1, 15, 9/9
NGC 513		0.01954	0.0035	0.82	5.0	0.48	0.41	1.32	53.7	...	...		18, 23/
NGC 5506		0.00618	0.045	0.916	7.20	4.24	8.44	9.24	355	10.8	340.	150	15, 24/9
NGC 5995	MCG −2-40-4	0.02443	0.0074	0.79	19.5	1.45	4.09	7.06	30.7	1.75	...	240	3P/25, 8
NGC 6552		0.0265	0.028	0.90	5.42	1.17	2.57	2.79	34.3	0.21	6000.	900	3P/9
NGC 7674[b]	Mrk 533	0.02906	0.049	1.02	4.80	1.79	5.64	8.46	220.0	0.05	100000	900	17, 18/9
NGC 7682[c]		0.0171	0.023	0.97	4.47	0.22	0.47	0.41	61.0	<1.3	...		3P, 15, 26/2
Tol 1238−364	IC 3639	0.01092	0.0457	0.89	5.56	2.63	9.08	14.03	79.6	0.025	100000	4200	27, 24/28, 25,8
Non-HBLR Seyfert 2 Galaxies													
F00198−7926		0.07280	0.0012	0.47	6.41	1.15	3.10	2.87	5.4[a]	<0.01	10000		8, 4/13
F03362−1642		0.03725	0.0005	0.73	8.1	0.35	1.02	2.01	9.3	...	...		3L, 4, 12/
F19254−7445	Super-Antennae	0.06171	0.0016	0.77	...	1.35	5.24	8.03	50[a]	0.025	2000		27, 29/30
M51	NGC 5194	0.00154	0.011	0.95	8.33	17.5	108.7	292.1	430.3	0.25	7500	1100	3L, 31/9
Mrk 266 SW[b]	NGC 5256	0.02778	0.0032	0.57	7.02	1.13	7.27	10.07	130.1	0.053	100000	575	3L, 15, 26/13
Mrk 573[c]		0.0173	0.160	1.01	3.90	0.81	3.60	1.3	20.5	<0.52	...		3L, 15, 26/2
Mrk 938	NGC 34	0.01978	0.0021	0.556	24.5	2.51	16.84	17.61	67.5	<0.39	1000		3P, 27, 7/2
NGC 1144[b]		0.02885	0.010	0.88	4.49	0.62	5.35	11.60	146.0	<1.21	100		3P, 27, 26, 7, 32/2
NGC 1241		0.01351	0.0037	0.74	8.9	0.60	4.37	10.74	167.9	...	...		3P, 32/
NGC 1320	Mrk 607	0.0094	0.014	0.97	4.86	1.32	2.21	2.82	6.5	<0.82	...		3L, 33/2
NGC 1386		0.00290	0.095	1.21	5.70	1.46	6.01	9.67	37.8	0.02	100000	7600	20, 34/9
NGC 1667		0.01517	0.0138	0.88	9.74	0.67	6.29	15.83	77.3	0.0026	10000.	<3000	3L, 35, 31/9
NGC 3079		0.00375	0.00018	0.62	25.0	3.65	50.95	105.2	808.0	0.06	160.		3L, 31/9
NGC 3362[c]		0.0276	0.007	0.92	3.69	0.35	2.13	3.16	15.2	<1.26	...		3L, 26, 2/2
NGC 3660		0.0122	0.0034	0.52	8.79	0.64	2.03	4.47	14.8	0.25	...		3L, 36, 24, 37/25
NGC 3982[b]		0.00370	0.020	1.24	4.5	0.97	7.21	16.78	50.1	<0.42	...		3L/2
NGC 4501		0.00761	0.0037	0.725	3.51	3.02	19.93	63.64	289.0	0.059	...		3L, 31/38
NGC 4941		0.00370	0.042	1.13	6.80	0.46	1.87	4.79	20.3	0.30	4500.	1600	20, 9/9
NGC 5135		0.01372	0.040	0.64	7.80	2.39	16.60	31.18	191.6	0.02	10000.	<11700	27, 15, 24, 32/9
NGC 5283[c]	Mrk 270	0.0104	0.027	0.79	3.1	0.13	0.21	0.27	12.8	<1.02	...		3L, 15, 26/2
NGC 5347[b]		0.00779	0.005	1.08	8.7	0.96	1.42	2.64	6.4	0.020	10000		3L, 39/28, 25

TABLE 1—*Continued*

Name	Other ID	z	$f_{[\mathrm{O\,III}]}$	[O III]/Hβ	Hα/Hβ	f_{25}	f_{60}	f_{100}	$S_{20\,\mathrm{cm}}$	HX	N_H	EW(Fe)	Reference
NGC 5695[c]	Mrk 686	0.014	0.007	0.92	3.1	0.129	0.566	1.79	6.6	<0.01	...		3L, 26, 2/2
NGC 5929[b]		0.00831	0.0093	0.57	5.32	1.67	9.52	13.84	100.0	<0.79	...		3P, 15, 26/2
NGC 6890		0.00807	0.019	0.985	4.69	0.80	4.01	8.26	10.0[a]	...	...		20, 15, 28, 40/
NGC 7172		0.00868	0.004	0.97	3.0	0.95	5.74	12.43	29.9	2.14	861.	121	27, 41, 32/9
NGC 7582		0.00525	0.043	0.46	7.60	7.48	52.47	83.27	166.0	2.72	1240.	182	27, 15, 24/9
UGC 6100[c]	A1058+45	0.0295	0.029	1.14	4.50	0.28	0.81	1.96	10.5	<1.14	...		3L, 26, 42/2
LINER, H II, and Starburst Galaxies													
Arp 220	UGC 9913	0.01813	0.00014	0.01	9.09	8.06	107.3	120.2	327.6	0.022	60.	<600	3P, 43/44
F08572+3915		0.05821	0.00012	0.36	14.6	1.87	7.33	4.98	4.9	<0.007	10000		3K, 7, 43/13
F23461+0157	CGCG 381-051	0.03060	0.0019	−0.60	6.00	0.18	1.75	2.76	5.5	...	...		3P/
MCG +0-29-23		0.02490	0.00053	0.07	12.3	0.68	5.93	9.48	35.3	1.96	...		3L, 7/2
Mrk 273		0.03778	0.0033	0.45	9.33	2.30	22.80	22.20	138.7	0.35	4902	342	7, 16/9
Mrk 461[c]		0.0162	0.00089	0.13	7.70	0.124	0.375	0.46	6.6	<1.17	...		3L/2
Mrk 897	UGC 11680	0.02634	0.0024	−0.22	5.32	0.86	2.97	5.59	17.3	...	...		3P/
Mrk 1183	NGC 1056	0.00515	0.00228	−0.14	6.61	0.48	5.49	10.22	38.5	...	...		7/
NGC 1097		0.00425	0.00184	0.58	>7	7.70	46.73	116.3	227.1	0.17	13.	<300	35, 45/46
NGC 4922		0.023	0.00265	0.43	7.08	1.52	6.18	7.69	39.3	...	...		3L, 7/
NGC 5005		0.00316	0.00473	0.356	2.59	2.31	22.41	63.73	182.7	0.072	...		47, 31/38
NGC 5953		0.00656	0.00486	0.26	7.59	1.67	11.85	20.47	97.3	...	...		7, 28/
NGC 6810		0.00677	0.0013	−0.25	10.9	3.61	18.90	33.30	...	2.06	...		48, 49/2
NGC 7130	IC 5135	0.01440	0.0341	0.38	8.36	2.15	16.85	26.96	178.6	0.05	10000.		27, 7, 24/13, 28
NGC 7496		0.00550	0.00661	−0.22	6.10	2.00	10.21	16.59	36.3	<0.8	501		27, 24, 1, 32/2, 50
NGC 7590		0.00532	0.0033	0.0	5.40	0.94	7.81	21.05	57.5	0.12	<9.2		27, 24/9

Notes.—The 14 S2s with footnote references b and c comprise the CfA S2 sample. The rest come from the 12 μm sample. The term $f_{[\mathrm{O\,III}]}$ is the observed [O III] λ5007 flux, uncorrected for extinction, in units of 10^{-11} ergs s^{-1} cm^{-2}. [O III]/Hβ is the logarithmic narrow emission-line ratio corrected for reddening. *IRAS* fluxes f_{25}, f_{60}, and f_{100} (in Jy) are drawn, in order of preference, from Rush et al. 1993, the *IRAS* Faint Source Catalog, and Pérez García & Rodríguez Espinosa 2001. The radio 20 cm flux density $S_{20\,\mathrm{cm}}$ (in mJy) is drawn mainly from the NVSS survey (Condon et al. 1998), Rush, Malkan, & Edelson 1996, and the FIRST survey (Becker, White, & Helfand 1995). HX is the hard X-ray (2–10 keV) flux corrected for absorption, in units of 10^{-11} ergs s^{-1} cm^{-2}. The term N_H is the column density in units of 10^{20} cm^{-2}. EW(Fe) is the Fe Kα equivalent width in eV. References for HBLR and non-HBLR properties are given in the first half of the "Reference" column (before the slash), along with those for the [O III] flux and Balmer decrement. Those for the X-ray [HX, N_H, and EW(Fe)] properties are given in the second half (after the slash). The following S2s from the 12 μm sample have no spectropolarimetric data: ESO 541–IG 12, ESO 33–G2, ESO 253–G3, MCG −4-2-18, NGC 1125, NGC 3147, NGC 3822, and NGC 4968.

[a] Flux density $S_{20\,\mathrm{cm}}$ is from Ulvestad & Wilson 1989 for NGC 6890. For F00521, F00198, and F19254, $S_{20\,\mathrm{cm}}$ is extrapolated from $S_{2.3\,\mathrm{GHz}}$ (Roy et al. 1994) assuming $S_\nu \propto \nu^{-0.7}$.

[b] Object is in both the CfA and 12 μm samples.

[c] Object is in the CfA sample only.

References.—(1) Young et al. 1996b; (2) Polletta et al. 1996; (3) This work and telescope (K=Keck, L=Lick, P=Palomar); (4) de Grijp et al. 1992; (5) Heisler, Vader, & Frogel 1989; (6) Dopita et al. 1998; (7) Veilleux et al. 1995; (8) Lumsden et al. 2001; (9) Bassani et al. 1999; (10) Severgnini et al. 2001; (11) Osterbrock & de Robertis 1985; (12) Lipari, Bonatto, & Pastoriza 1991; (13) Risaliti et al. 2000; (14) Inglis et al. 1993; (15) Whittle 1992; (16) Dahari & de Robertis 1988; (17) Miller & Goodrich 1990; (18) Tran 1995; (19) Miller & Antonucci 1983; (20) Moran et al. 2000; (21) Murayama, Taniguchi, & Iwasawa 1998; (22) Collinge & Brandt 2000; (23) Tran et al. 1992a; (24) Storchi-Bergmann, Kinney, & Challis 1995; (25) TARTARUS database of *ASCA* observations of AGNs (available at http://tartarus.gsfc.nasa.gov); (26) OM93; (27) Heisler et al. 1997; (28) Risaliti, Maiolino, & Salvati 1999; (29) Duc, Mirabel, & Maza 1997; (30) Pappa, Georgantopoulos, & Stewart 2000; (31) Ho, Filippenko, & Sargent 1997; (32) Vaceli et al. 1997; (33) de Robertis & Osterbrock 1986; (34) Storchi-Bergmann & Pastoriza 1989; (35) Barth et al. 1999; (36) Kollatschny et al. 1983; (37) Gonçalves, Véron-Cetty, & Véron 1999; (38) Terashima, Ho, & Ptak 2000; (39) González Delgado & Pérez 1996; (40) Storchi-Bergmann, Bica, & Pastoriza 1990; (41) Coziol et al. 1998; (42) Cruz-Gonzalez et al. 1994; (43) Veilleux, Kim, & Sanders 1999; (44) Iwasawa et al. 2001; (45) Storchi-Bergmann, Baldwin, & Wilson 1993; (46) Iyomoto et al. 1996; (47) A. J. Barth 2000, private communication; (48) Kirhakos & Steiner 1990; (49) Véron-Cetty & Véron 1986; (50) Kruper, Urry, & Canizares 1990.

TABLE 2

SEYFERT 1 GALAXIES OF THE CfA AND 12 μm SAMPLES

Name	Other ID	z	$f_{[\mathrm{O\,III}]}$	[O III]/Hβ	f_{25}	f_{60}	f_{100}	$S_{20\,\mathrm{cm}}$	Reference
A0048+29[a]	UGC 524	0.0360	...	...	0.165	0.944	1.72	11.4	
E12–G21		0.03002	0.0097	...	0.25	1.45	2.98	...	1
E141–G55		0.03600	0.023	...	0.46	0.47	1.48	<36	2, 1
F03450+0055		0.03100	0.010	...	0.39	0.87	3.92	32.0	3
F05563-3820		0.03387	0.0075	...	0.77	0.38	0.56	34.6	4
F13349+2438		0.10764	0.0047	...	0.72	0.85	0.90	19.6	5
F15091-2107		0.04461	0.020	...	0.97	1.60	1.49	46.9	1, 6
IC 4329A		0.01605	0.034	0.71	2.26	2.15	2.31	66.4	2, 7
I Zw 1[b]		0.0611	0.0044	...	1.17	2.24	2.87	8.8	6
MCG −2-33-34	NGC 4748	0.01463	0.025	0.72	0.65	1.23	2.36	14.0	4
MCG −3-7-11	MBG 02223-1922	0.03373	0.0244	1.21	0.35	1.45	3.65	31.5	8
MCG −5-13-17		0.01264	0.039	1.32	0.57	1.28	2.34	14.2	1, 4
MCG −6-30-15		0.00775	0.010	...	0.97	1.39	2.26	29.5	1
Mrk 6		0.01881	0.075	1.10	0.73	1.25	0.90	268.4	2, 6
Mrk 9		0.03987	0.0109	...	0.39	0.76	0.98	3.6	2
Mrk 79		0.02219	0.037	1.089	0.73	1.55	2.35	20.5	2, 6
Mrk 205[a]		0.07085	0.0058	...	0.080	0.29	1.31	6.1	6
Mrk 231[b,c]		0.04217	0.023	...	8.80	35.4	32.28	308.9	6
Mrk 279[a]		0.03045	0.012	0.627	0.50	1.58	2.31	23.2	2, 6, 9
Mrk 335[b]		0.0258	0.023	...	0.45	0.35	0.57	7.6	2
Mrk 509		0.03440	0.081	0.95	0.73	1.39	1.36	18.6	2, 6
Mrk 618		0.03555	0.013	...	0.85	2.70	4.16	17.0	2
Mrk 704		0.02923	0.013	0.80	0.60	0.36	0.45	6.1	2, 9
Mrk 817[b]		0.03145	0.014	1.217	1.42	2.33	2.35	11.2	2, 6
Mrk 841[a]		0.03620	0.025	1.10	0.46	0.47	0.30	<14.8	6, 9
Mrk 993[a]		0.0155	0.003	0.80	0.09	0.34	1.25	5.9	6, 10
Mrk 1239		0.01993	0.024	...	1.21	1.41	1.07	62.2	2, 6
NGC 863[a]	Mrk 590	0.0264	0.0053	...	0.221	0.489	1.46	16.8	6
NGC 931	Mrk 1040	0.01665	0.013	0.757	1.42	2.80	5.66	15.4	2, 6
NGC 1566		0.00499	0.030	1.065	3.07	23.12	58.72	...	2, 6
NGC 2992		0.00771	0.036	1.00	1.37	6.87	14.44	226.2	6
NGC 3080[a]	Mrk 1243	0.0354	0.0013	...	<0.153	0.349	0.874	2.9	6
NGC 3227[b]		0.00386	0.073	1.206	1.88	8.45	17.93	97.5	2, 6
NGC 3516[b]		0.00884	0.038	1.13	0.96	2.09	2.73	31.3	2, 6
NGC 4051[b]		0.00242	0.046	...	2.28	10.62	25.10	94.4	2, 6
NGC 4151[b]		0.00332	0.980	1.15	5.04	5.64	8.50	359.6	2, 6
NGC 4235[a]		0.00804	0.0025	1.11	0.28	0.65	0.66	12.2	6, 9
NGC 4253[b]	Mrk 766	0.01293	0.063	...	1.47	3.89	4.20	38.1	2, 6
NGC 4593	Mrk 1330	0.0090	0.017	1.12	0.96	3.43	6.26	4.4	2, 6
NGC 5548[b]		0.01717	0.054	1.12	0.81	1.07	2.07	28.2	2, 6
NGC 5940[a]		0.03393	0.0035	...	0.112	0.74	1.75	8.8	11
NGC 6104[a]		0.02811	...	...	0.16	0.76	0.90	6.4	
NGC 6860		0.01488	0.021	0.60	0.31	0.96	2.19	...	12
NGC 7213		0.00598	0.0377	0.54	0.81	2.70	8.99	145[d]	13
NGC 7469[b]		0.01632	0.071	0.778	6.04	28.57	35.83	180.5	2, 6
NGC 7603[b]	Mrk 530	0.02952	0.039	1.064	0.191	0.856	2.14	24.4	2, 6

NOTES.—The term $f_{[\mathrm{O\,III}]}$ is the observed [O III] λ5007 flux, uncorrected for extinction in units of 10^{-11} ergs s^{-1} cm^{-2}. [O III]/Hβ is the logarithmic emission-line ratio corrected for reddening and refers to the *narrow* components only. *IRAS* fluxes f_{25}, f_{60}, and f_{100} (in Jy) are drawn, in order of preference, from Rush et al. 1993, the *IRAS* Faint Source Catalog, Edelson, Malkan, & Rieke 1987, and Pérez García & Rodríguez Espinosa 2001. The radio 20 cm flux density $S_{20\,\mathrm{cm}}$ (in mJy) is drawn mainly from the NVSS survey (Condon et al. 1998), Rush et al. 1996, and the FIRST survey (Becker et al. 1995). References for [O III] flux properties are given in the last column. The following powerful radio galaxies/quasars have been excluded from the S1 list of Rush et al. 1993: 3C 120, 3C 234, 3C 273, and 3C 445.

[a] Object is in the CfA sample only.

[b] Object is in both the CfA and 12 μm samples.

[c] *IRAS* fluxes are from Soifer et al. 1989.

[d] Flux density $S_{20\,\mathrm{cm}}$ is extracted from fluxes at 2.3 and 8.4 GHz from Slee et al. 1994.

REFERENCES.—(1) Winkler 1992; (2) Whittle 1992; (3) Boroson & Meyers 1992; (4) Rodríguez-Ardila, Pastoriza, & Donzelli 2000; (5) Wills et al. 1992; (6) Dahari & de Robertis 1988; (7) Pastoriza 1979; (8) Coziol et al. 1993; (9) Cohen 1983; (10) Tran, Osterbrock, & Martel 1992b; (11) Bonatto & Pastoriza 1997; (12) Lipari, Tsvetanov, & Macchetto 1993; (13) Filippenko & Halpern 1984.

paper (such as NGC 5347 and NGC 5929) may turn out to show weak polarized broad lines. However, as we show in the rest of this paper, the majority of the non-HBLR S2s are probably real S2s that may not contain a genuine S1 nucleus. This is based mainly on the finding that their large-scale properties are systematically different from both HBLR S2s and normal S1s, showing that they cannot be the same type of objects seen from another direction. This is in contrast to the HBLR S2s, which are true S1 counterparts and whose properties match those of S1s.

Although many of the HBLR S2s detected by optical spectropolarimetry have also been observed to show broad permitted lines directly in near-IR spectroscopy, which presumably probes deeper through the obscuring torus, the correspondence of BLR detection between the two different methods is generally poor (e.g., Veilleux, Goodrich, & Hill 1997; Lutz et al. 2003). The rate of BLR detection in S2s by direct near-IR spectroscopy is around 25%, somewhat lower than that by spectropolarimetry, and many of the S2s known to have polarized optical broad lines fail to show a corresponding near-IR broad line, such as Brα, in direct flux (Lutz et al. 2003). These results imply that in some S2s the obscuring material is still considerably optically thick at $\sim$4 μm.

2.2. *Diagnostic Diagrams and Luminosity Distributions*

In order to compare various properties among the HBLR and non-HBLR S2s and S1s, we now present several diagnostic diagrams that aim to illustrate their similarities and differences. The results of our statistical tests are summarized in Table 3. We first examine the [O III]/Hβ versus f_{25}/f_{60} plot shown in Figure 1. As discussed in Paper I, these two ratios display significant differences between the two S2 classes. What remains to be determined is how they compare to the S1 population. In considering the S1s, we must keep in mind that the [O III]/Hβ ratio refers only to the narrow-line component. Thus, strictly speaking, only type 1 Seyferts that show a prominent Hβ narrow component, such as Seyfert 1.5s, should be considered. Thus, we have gathered the relevant data from the literature for S1.5s, which are listed in Table 2 and plotted in Figure 1, along with those for both HBLR and non-HBLR S2s. The distributions of [O III]/Hβ and f_{25}/f_{60} as a function of Seyfert types are shown in Figures 2 and 3. A visual examination quickly confirms that indeed S1.5s do tend to show [O III]/Hβ and f_{25}/f_{60} ratios similar to HBLR S2s, suggesting that

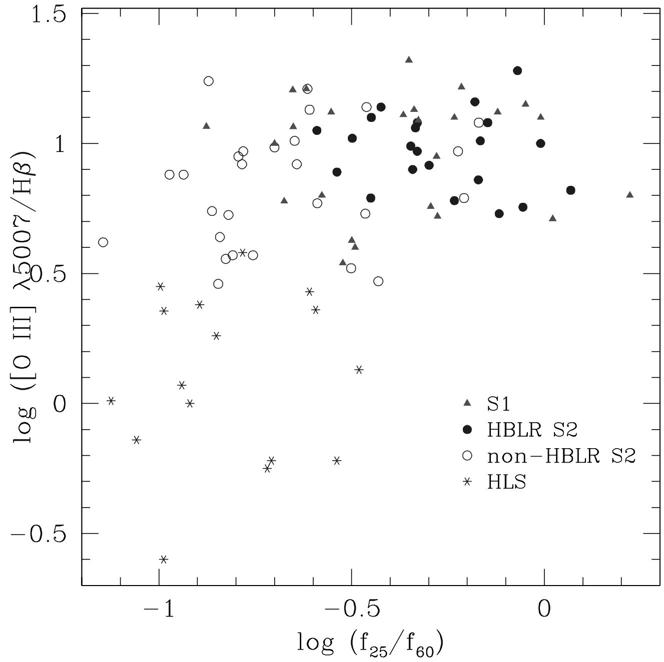

FIG. 1.—Ionization measure [O III]/Hβ vs. IR color f_{25}/f_{60} for the CfA and 12 μm samples. S1s are shown as filled triangles, HBLR S2s as filled circles, and non-HBLR S2s as open circles. Asterisks denote HLS galaxies, all of which have no HBLRs. [*See the electronic edition of the Journal for a color version of this figure.*]

they are intrinsically the same type of object. A formal Kolmogorov-Smirnov (K-S) test shows that statistically the mean [O III]/Hβ and f_{25}/f_{60} ratios for the S1.5s are not significantly different from those shown by the HBLR S2s (Table 3).[4] Compared to non-HBLR S2s, however, the

[4] We adopt the traditional view that a test result with $p_{\rm null} \leq 5\%$ is considered to be significant.

TABLE 3
STATISTICAL PROPERTIES OF S1, HBLR S2, AND NON-HBLR S2 GALAXIES

	SEYFERT 1 (S1)			HBLR S2 (S3)			NON-HBLR S2 (S2)			K-S $p_{\rm null}$			
PROPERTY[a] (1)	N (2)	Mean (3)	σ (4)	N (5)	Mean (6)	σ (7)	N (8)	Mean (9)	σ (10)	S1-S3 (11)	S1-S2 (12)	S3-S2 (13)	INDICATOR (14)
log([O III]/Hβ)	25	0.971	0.223	22	0.972	0.145	27	0.831	0.230	24.9	3.6	6.3	AGN strength
log(f_{25}/f_{60})	46	−0.368	0.281	22	−0.273	0.179	27	−0.678	0.239	13.6	0.079	0.0008	AGN strength
log(S_{20}/f_{60})	43	−1.77	0.409	22	−1.55	0.60	27	−2.07	0.358	11.1	1.1	0.8	AGN strength
log L([O III])[b]	44	7.56	0.637	22	7.56	0.780	26	6.85	0.703	94.8	0.016	0.36	AGN strength
log L_{25}	46	10.2	0.660	22	10.6	0.506	27	9.92	0.735	8.8	26.2	0.23	AGN strength
log $L_{\rm rad}$	43	3.37	0.668	22	3.87	0.597	27	3.10	0.824	4.5	15.5	1.5	AGN strength
log $L_{\rm FIR}$	46	10.2	0.614	22	10.5	0.564	27	10.3	0.765	12.7	52.5	58.2	SF activity
log(HX/[O III])[c]	...	...	...	15	0.330	0.915	13	−0.196	0.971	...	...	36.5	Obscuration
log[EW(Fe)][d]	...	...	...	13	2.63	0.139	08	2.84	0.231	...	...	57–68	Obscuration
log($N_{\rm H}$)[d]	...	...	...	13	23.84	0.24	14	23.86	0.29	...	...	88–100	Obscuration
Hα/Hβ	...	...	...	23	7.16	4.7	26	7.39	5.51	...	...	36	Obscuration

NOTES.—Col. (1): Observational property being compared. Cols. (2)–(10): For each sample of S1, HBLR S2, and non-HBLR S2 galaxies, N is the number of data points, "Mean" is the mean, and σ is the standard deviation from the mean. Col. (11): From the K-S test of S1s (S1) vs. HBLR S2s (S3), the probability $p_{\rm null}$ (in percent) for the null hypothesis that the two distributions are drawn at random from the same parent population. Col. (12): As in col. (11), but for S1s vs. non-HBLR S2s (S2). Col. (13): As in col. (11), but for HBLR S2s vs. non-HBLR S2s. Col. (14): A rough indication of what the quantity under consideration represents.

[a] All luminosities are in units of $L_\odot$; EW(Fe) is in eV; $N_{\rm H}$ is in cm^{-2}.

[b] Outlier NGC 3079 is excluded in the non-HBLR S2 sample.

[c] Detections only.

[d] Statistical tests include Gehan's permutation variance, Gehan's hypergeometric variance, log rank, Peto and Peto, and Peto and Prentice.

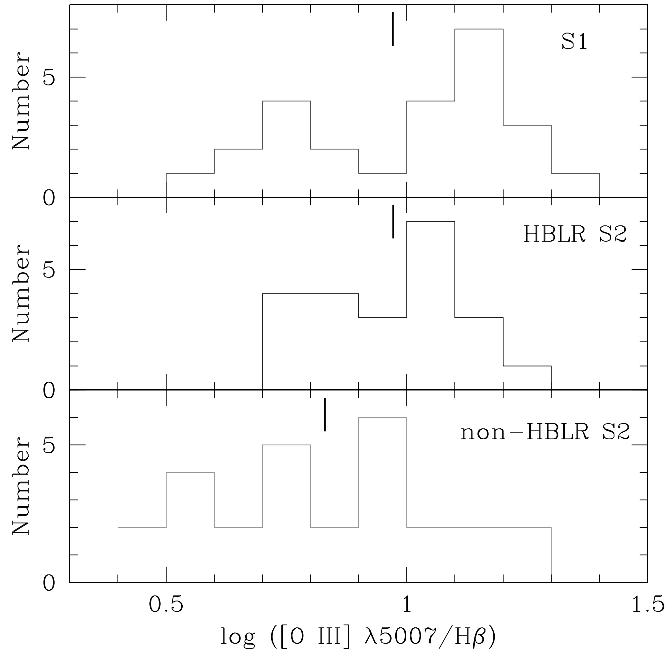

FIG. 2.—Distribution of [O III]/Hβ ratio for the combined CfA and 12 μm samples of S1s (*top*), HBLR S2s (*middle*), and non-HBLR S2s (*bottom*). The vertical tick mark in each panel denotes the mean of each distribution. The S1s show a distribution similar to that of HBLR S2s, both of which are significantly different from that of non-HBLR S2s. [*See the electronic edition of the Journal for a color version of this figure.*]

S1.5s display significantly higher values of these quantities. Thus, not only are non-HBLR S2s different from HBLR S2s; the latter appear to be similar to normal S1s. These results provide additional support for the concept put forward in Paper I that the two types of S2s are different, with one being truly obscured S1s and the other having much less powerful central AGNs.

Note in Figure 1 that the lower right corner can be populated by HBLRs, indicating that not all S2s with a low [O III]/Hβ ratio are necessarily non-HBLRs. This could be explained as a result of a combination of obscuration of the NLR and mixing of starburst and AGN components (e.g., see Hill et al. 2001; Levenson et al. 2001a). The lower line ratio could also arise in part from partial obscuration either by the obscuring torus or dust of the higher ionization lines close to the nucleus. Evidence for such obscuration has come from the observation of stratification of the polarization of narrow emission lines, in the sense that higher ionization lines have higher polarization (Barth et al. 1999; Tran et al. 2000). The f_{25}/f_{60} ratio, however, is not significantly affected by the obscuration, maintaining an essentially warm color. Thus, HBLR S2s lying in this region are likely to be dusty S2 galaxies with a mixed starburst component, having extended dust lanes that could obscure much of the high-ionization optical emission close to the nucleus.

We turn next to the diagram of $S_{20\,\mathrm{cm}}/f_{60}$ versus f_{25}/f_{60}, which has been shown in Paper I to display a markedly clear segregation between S2 types. In Figure 4 we add in the S1 data. Again, the S1s show a strong tendency to lay among the HBLR S2s and to avoid the region inhabited by non-HBLR S2s. The distributions of $S_{20\,\mathrm{cm}}/f_{60}$ (Fig. 5) confirm these behaviors, and K-S tests show that S1s and HBLR S2s are statistically alike, with both being significantly different from the non-HBLR S2s (Table 3). Note that most of the radio data used come from the 1.5 GHz NRAO VLA Sky Survey (NVSS). Higher resolution data for both samples are available at 8.3 GHz (Thean et al. 2000, 2001; Kukula et al. 1995), but the shorter wavelength radio emission may have a higher contribution from star formation in the host. In addition, since we are considering the ratio of radio flux

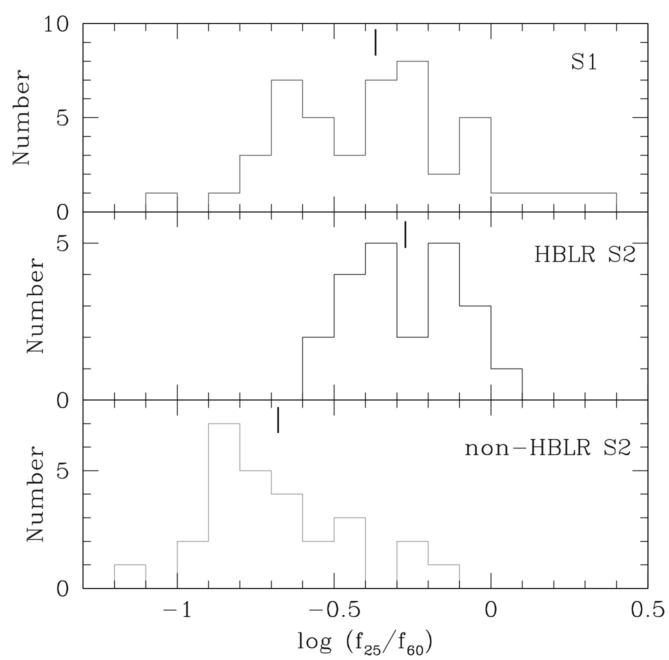

FIG. 3.—Distributions of the IR color ratio f_{25}/f_{60}, arranged as in Fig. 2. The S1s show a distribution similar to that of HBLR S2s, both of which are significantly different from that of non-HBLR S2s. [*See the electronic edition of the Journal for a color version of this figure.*]

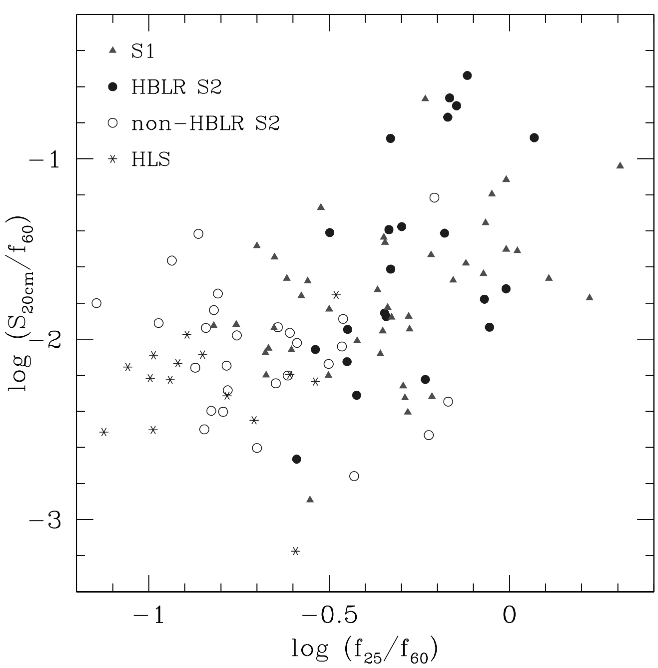

FIG. 4.—The 20 cm radio flux density $S_{20\,\mathrm{cm}}$, normalized by the FIR flux f_{60}, which is dominated by star formation in the host galaxy, as a function of IR color f_{25}/f_{60} for the CfA and 12 μm samples. Symbols are as in Fig. 1. [*See the electronic edition of the Journal for a color version of this figure.*]

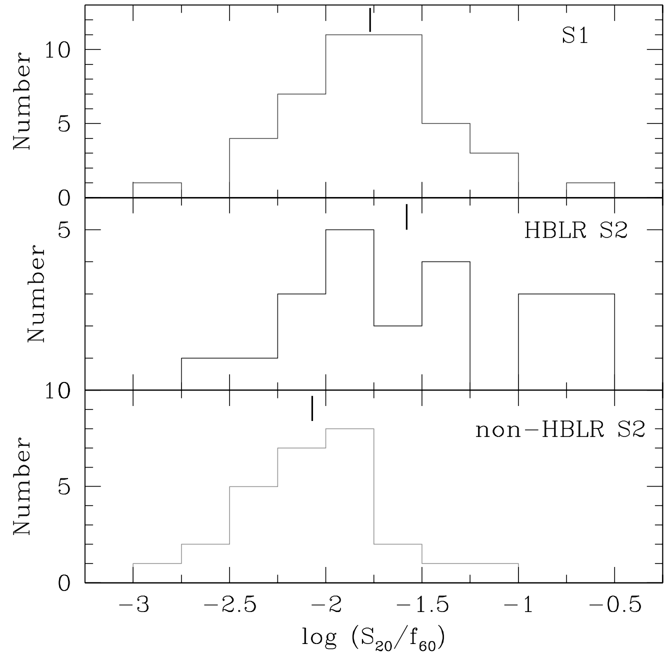

FIG. 5.—Distributions of the $S_{20\,\mathrm{cm}}/f_{60}$ ratio, arranged as in Fig. 2. The S1s show a distribution similar to that of HBLR S2s, both of which are significantly stronger than that of non-HBLR S2s. [*See the electronic edition of the Journal for a color version of this figure.*]

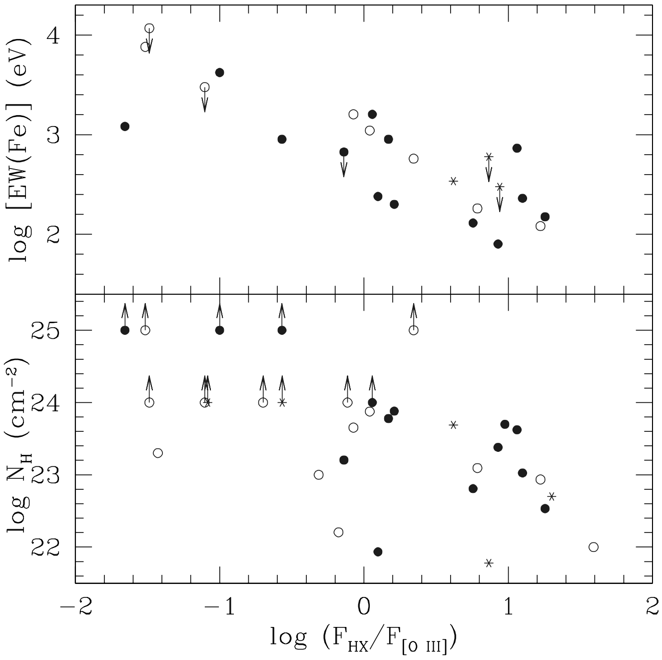

FIG. 6.—HX/[O III] ratio vs. absorbing column density N_{H} and EW of the Kα Fe emission line for S2s and HLS galaxies in the 12 μm sample. Symbols are as in Fig. 1; arrows denote upper or lower limits. There is a good anticorrelation between HX/[O III] and both N_{H} and EW(Fe), indicating that these parameters can be used as measures of the nuclear obscuration. [*See the electronic edition of the Journal for a color version of this figure.*]

to *IRAS* far-IR (FIR) flux, which is more comparable to NVSS resolution, the NVSS data would be more appropriate for this purpose. By normalizing to the FIR, which is dominated by extended star formation, much of the non-nuclear radio emission has been accounted for, and the nuclear contribution has, in effect, been isolated. Using their high-resolution 8.3 GHz data, Thean et al. (2001) have also done a comparison of radio power between S1s and the two S2 subtypes. Their results are basically consistent with ours in finding that the HBLRs are more powerful in the radio than non-HBLRs (see below), suggesting that the difference in resolution in the radio data does not have any significant impact on the results.

Paper I has shown that the mean hard X-ray (HX) column density as well as the Balmer decrement between non-HBLR and HBLR S2s are not significantly different, indicating their similarity in nuclear obscuration. To further examine if obscuration plays a role in the detection/visibility of HBLRs in S2s, we wish to explore other potential measures of obscuration. HX luminosity is reflective of the strength of the AGN, but it is also sensitive to obscuration. In order to isolate the effect of obscuration alone, we consider the ratio HX/[O III]. Since the [O III] strength is largely a measure of the strength of the AGN, by taking the ratio with [O III] we have effectively "divided out" the AGN component, leaving essentially a measure of obscuration. This ratio, called "T" in Bassani et al. (1999), has been shown to be a good indicator of obscuration (Bassani et al. 1999; Pappa et al. 2001). In particular, it is anticorrelated with both the column density N_{H} and the Kα iron-line equivalent width EW(Fe). In Figure 6, we plot N_{H} and EW(Fe) against HX/[O III] for our sample of 12 μm S2 galaxies. Both the HX and [O III] fluxes have been corrected for obscuration or extinction. We confirm that there appears to be a good anticorrelation between the HX/[O III] ratio and both N_{H} and EW(Fe) and that these quantities can be used as probes of the obscuration of the center of the active nucleus.

As shown in Figure 7, the distribution of HX/[O III] appears to be very similar between the two classes of HBLR and non-HBLR S2s. A K-S test of only the detected sources (no detection limits) shows that this ratio is virtually identical between HBLR and non-HBLR S2s ($p_{\mathrm{null}} = 36.5\%$). Taking into account censored (i.e., upper HX limits) data, however,[5] it appears to show that non-HBLR S2s may have a significantly ($p_{\mathrm{null}} = 3\%$–9%) higher obscuration than HBLR S2s. Better X-ray detections, perhaps with *Chandra* or *XMM-Newton*, may be able to confirm this difference. Turning to the EW(Fe), statistical tests also confirm that there is virtually no difference between the samples of 13 HBLR S2s and eight non-HBLR S2s ($p_{\mathrm{null}} = 57\%$–68%) with available data, which are plotted in Figure 6. Therefore, after examining various possible observational indicators for it, we conclude that the level of obscuration is largely indistinguishable between the two types of S2s, confirming the suggestion of Paper I that it does not play a great role in the detectability/visibility of HBLRs.

We next consider HX versus [O III] luminosities, shown in Figure 8. The diagram can be divided into four quadrants with the dividing lines roughly at $L(\mathrm{HX}) = 10^{42.4}$ ergs s^{-1} and $L([\mathrm{O\ III}]) = 10^{41.5}$ ergs s^{-1}. There is a good positive correlation between these two quantities, as would be expected, but there is also considerable scatter, which could arise from two sources: variability in the intrinsic X-ray flux or in absorbing column density (e.g., Risaliti, Elvis, & Nicastro

[5] Using the ASURV package in IRAF.

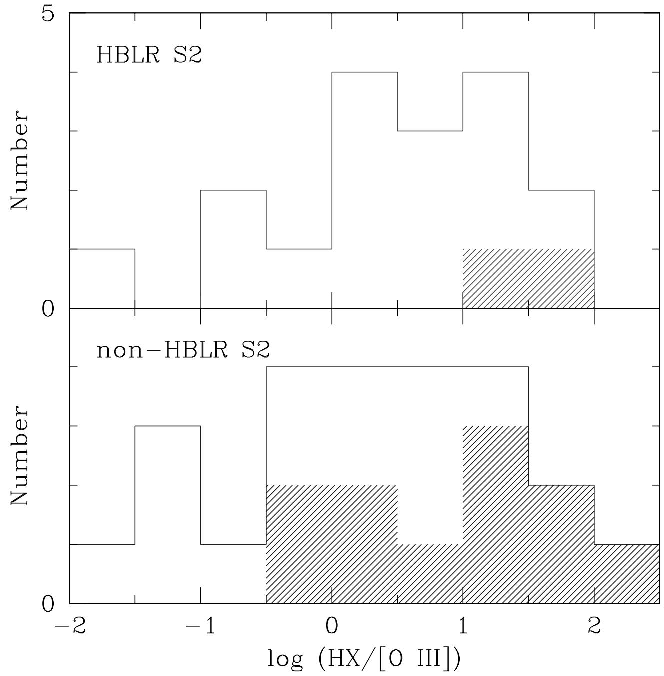

FIG. 7.—Distribution of the HX/[O III] ratio for HBLR S2s (*top*) and non-HBLR S2s (*bottom*) in the CfA and 12 μm samples. Shaded areas denote upper limits. Excluding detection limits, there is no significant difference in the mean HX/[O III] between HBLR and non-HBLR S2s, indicating that non-HBLR S2s are not any more obscured than HBLR S2s. Including the limits results in a modest significance in the difference between the two distributions. [*See the electronic edition of the Journal for a color version of this figure.*]

2002; Smith, Georgantopoulos, & Warwick 2001). In the upper right quadrant lie mainly the HBLRs; these are the strong AGNs with genuine hidden S1 nuclei. The lower right quadrant is occupied by similarly powerful AGNs with HBLRs, but these suffer from high obscuration; they are the so-called Compton-thick AGNs. All of the four labeled HBLR occupants in this quadrant (IC 3639, N424, N1068, and N7674) have $N_{\rm H} > 10^{24}$ cm^{-2}. The vast majority of the non-HBLRs lie in the lower left quadrant; these are the intrinsically weak AGNs. The lack of objects in the upper left quadrant is real: hard X-ray–luminous AGNs are not expected to show weak [O III]. This diagram shows that HBLRs and non-HBLRs can be well separated by their HX and [O III] luminosities.

Clear separation between the two S2 types is also seen in the L([O III]) versus f_{25}/f_{60} plot, shown in Figure 9, which is analogous to the stellar Hertzsprung-Russell diagram. Again, the positions of S1s in this "AGN H-R diagram" largely overlap those of HBLR S2s but not non-HBLR S2s. In the accompanying Figure 10, we show the distribution of log L([O III]) for the three Seyfert types: S1 and HBLR and non-HBLR S2s. Here, the observed [O III] luminosities uncorrected for extinction are shown. As can be seen, the distributions show a striking similarity between S1s and HBLR S2s, while there is a significant shift to lower values for the non-HBLR S2s. This result provides strong support for the UM in that it confirms the prediction that isotropic properties such as L([O III]) should be the same between S1s and S2s, *but only when the HBLR S2s are considered and non-HBLR S2s are excluded*. Keel et al. (1994) have noted the similar L([O III]) distributions for their sample of Seyfert galaxies selected on the basis of FIR flux and *warm* ($f_{25}/f_{60} > 0.27$) color. We can now understand why the S1s

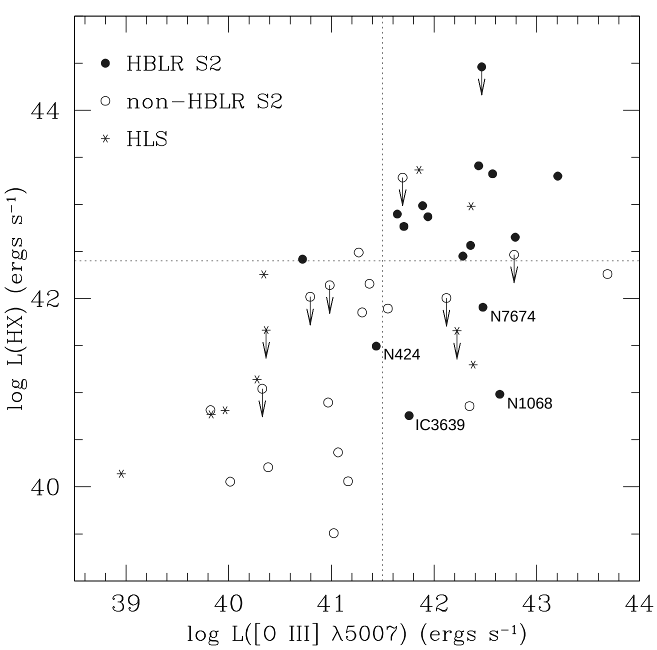

FIG. 8.—HX luminosity vs. optical [O III] λ5007 luminosity for CfA and 12 μm S2s. Symbols are as in Fig. 1. The dotted lines show the rough division between HBLR and non-HBLR S2s. Aside from the effect of absorption on the X-ray strength, there is a good correlation between L(HX) and L([O III]), with the HBLR S2s being stronger. [*See the electronic edition of the Journal for a color version of this figure.*]

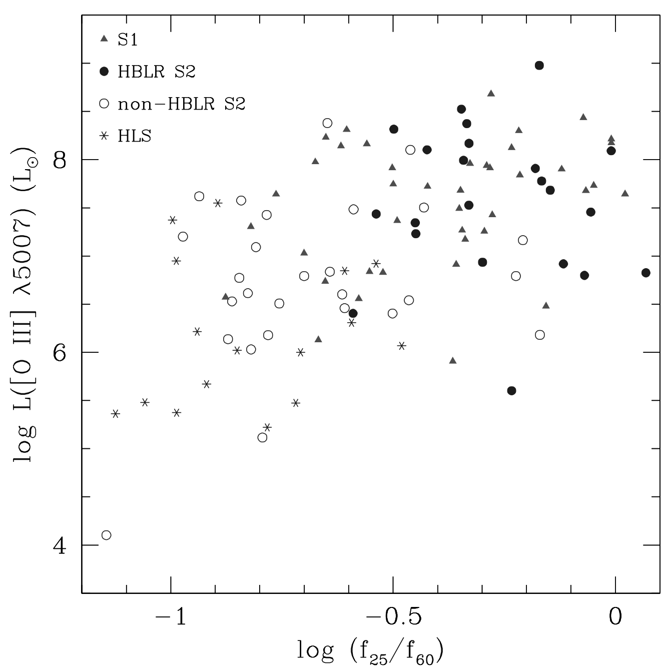

FIG. 9.—[O III] λ5007 luminosity vs. IR color f_{25}/f_{60} for the CfA and 12 μm samples. Symbols are as in Fig. 1. Good separation between HBLR and non-HBLR S2s is observed in this diagram. The S1s tend to lie among the HBLR S2s while largely avoiding the lower left corner, which is occupied mainly by non-HBLR S2s and HLS galaxies. [*See the electronic edition of the Journal for a color version of this figure.*]

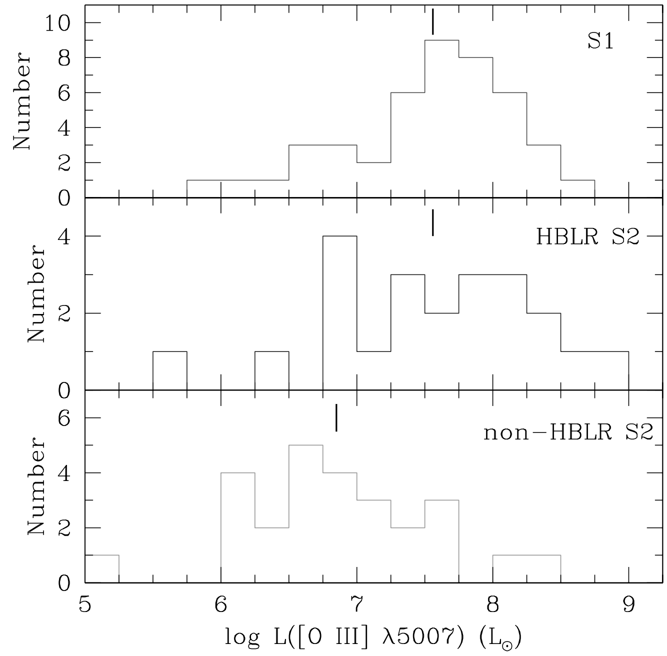

FIG. 10.—Distributions of [O III] luminosity in units of log solar luminosity, arranged as in Fig. 2. The S1s show a distribution similar to that of HBLR S2s, both of which are significantly stronger than that of non-HBLR S2s. [*See the electronic edition of the Journal for a color version of this figure.*]

and S2s in their sample are well matched in L([O III]): since warm S2s are well known to be largely of the HBLR variety, non-HBLR S2s have been selected against, and thus most if not all of the S2s in their sample are truly misdirected S1s. This point is considered further in § 3.2. When the separation of HBLR and non-HBLR S2s is not properly performed in the analysis, the combined sample of S2s will show a *smaller* average L([O III]) than S1s. This expectation is confirmed by our sample and also consistent with that implied by the results of Maiolino & Rieke (1995).

The distribution of L_{25} (Fig. 11) shows a behavior similar to that of L([O III]), but with lower significance. It confirms the result of Lumsden & Alexander (2001) that HBLR S2s are more energetic at mid-IR wavelengths than non-HBLR S2s. While the 25 μm luminosity of S1s seems to be similar to the former, however, they also share this property with the latter. Finally, in terms of radio power, it has been shown (Paper I; Moran et al. 1992; Thean et al. 2001) that HBLR S2s as a group are more luminous than their weaker, non-HBLR cousins. However, compared to S1s, HBLR S2s also appear significantly stronger, consistent with Thean et al. (2001), as Figure 12 and Table 3 show.

Turning to the FIR luminosity, we find the situation to be quite different. Following Condon et al. (1991), the FIR flux is calculated according to the formula $f_{\rm FIR} = 1.26 \times 10^{-14}(2.58 f_{60} + f_{100})$ W m^{-2}. As shown in Figure 13, the distribution of $L_{\rm FIR}$ is indistinguishable among the three Seyfert types, with a mean log $L_{\rm FIR}$ of about 10.3 $L_{\odot}$. Since the FIR luminosity is a good indicator of star-forming regions (e.g., Alonso-Herrero et al. 2001; Ruiz et al. 2001), this suggests that the circumnuclear star formation levels in these classes of Seyferts are essentially the same. The major implication is that the increased AGN power observed in S1s and HBLR S2s compared to non-HBLR S2s is due neither to the increased obscuration nor elevated level of star formation in the latter, both of which could effectively mask the AGN activity, but rather to the intrinsically stronger nuclear activity of the former. Our result is consistent with Pérez García & Rodríguez Espinosa (2001), who found that the cold (FIR) components in the CfA S1 and (total) S2 populations are similar. However, their finding that the

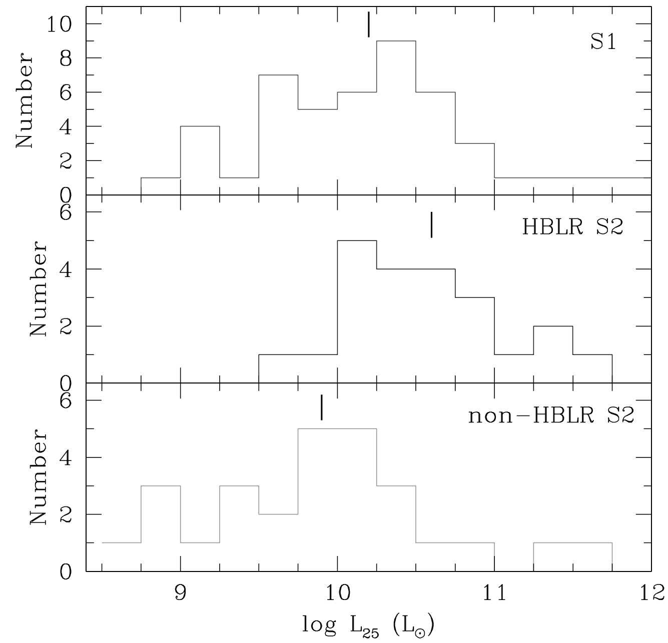

FIG. 11.—Distributions of *IRAS* 25 μm luminosity in units of log solar luminosity, arranged as in Fig. 2. [*See the electronic edition of the Journal for a color version of this figure.*]

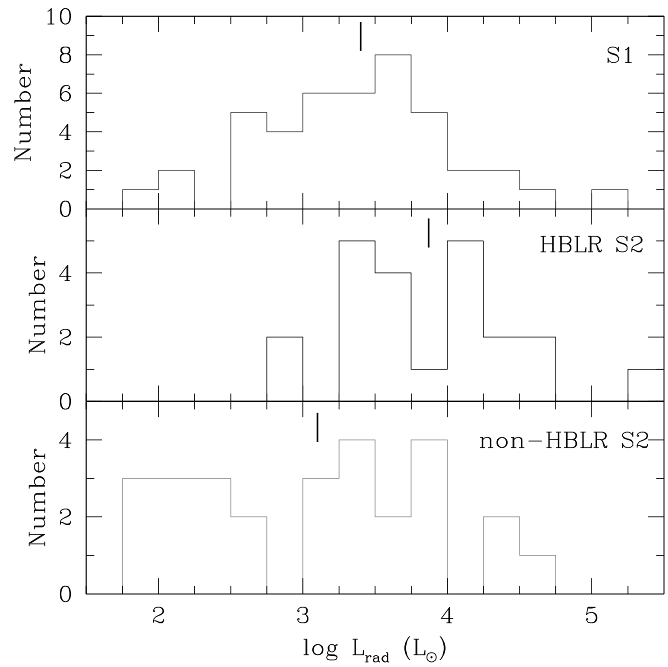

FIG. 12.—Distributions of 20 cm radio luminosity in units of log solar luminosity, arranged as in Fig. 2. Compared to non-HBLR S2s, HBLR S2s are more powerful in the radio, but the latter also appear to be more powerful than S1s. The radio luminosity has been calculated assuming a uniform bandwidth of 45 MHz. [*See the electronic edition of the Journal for a color version of this figure.*]

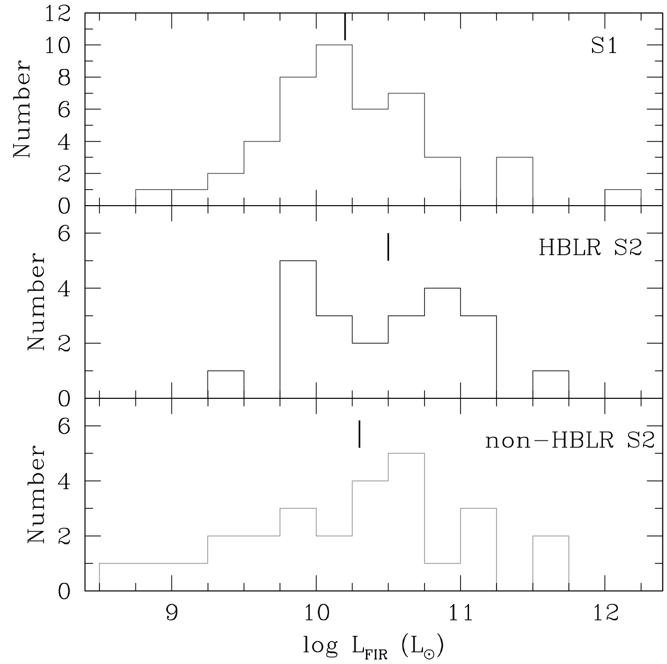

FIG. 13.—Distributions of FIR luminosity in units of log solar luminosity, arranged as in Fig. 2. The distributions for the three classes of Seyfert galaxies are statistically identical. [*See the electronic edition of the Journal for a color version of this figure.*]

warm (mid-IR) component in S1s is stronger than in S2s can be fully accounted for by the presence of non-HBLR S2s (see § 3.2).

In summary, we present in Table 4 a simple outline of the differences and similarities in the various observational properties discussed among the S1s and HBLR and non-HBLR S2s. For simplicity, in the table we denote HBLR S2s as S3s and non-HBLR S2s simply as S2s. Similarity is denoted by the "equals" or "approximately equals" symbols, and significant difference is indicated by the "greater than" sign. The results show that while obscuration and SF activity seem to be similar between the two S2 types, virtually all measures of AGN power indicate that non-HBLR S2s are different from and less energetic than HBLR S2s, which in turn appear to be the same as genuine S1s. Thus, only the HBLR S2s should strictly be considered truly S1s viewed from a different direction.

TABLE 4
COMPARISON BETWEEN S1, HBLR S2 (S3), AND NON-HBLR S2 (S2) GALAXIES

Property	Comparison
log([O III]/Hβ)	(S1 = S3) > S2
log(f_{25}/f_{60})	(S1 = S3) > S2
log(S_{20}/f_{60})	(S1 = S3) > S2
log L([O III])	(S1 = S3) > S2
log L_{25}	S1 ≈ S3 > S2 ≈ S1
log $L_{\rm rad}$	S3 > (S2 ≈ S1)
log $L_{\rm FIR}$	S1 = S3 = S2
log(HX/[O III])	S3 = S2
log[EW(Fe)]	S3 = S2
log($N_{\rm H}$)	S3 = S2
Hα/Hβ	S3 = S2

Note that even with the substantial reduction in the true number of hidden S1 nuclei (by roughly half), the real S2 model is not inconsistent with the observed size of the ionization cones of Seyfert galaxies. For a typical half-opening cone angle of $\approx 30°$ (e.g., Wilson & Tsvetanov 1994), the relative space number density of S2s to S1s is about 6.5:1. If the number of true hidden S1s (i.e., excluding the non-HBLR S2s) is cut by half, as our data suggest, then the torus half-opening angle would rise to $\sim 40°$. This is entirely within the range observed and fully consistent with existing data, given the inherent difficulty and uncertainty involved in measuring opening angles of ionization cones.

3. DISCUSSION

3.1. *Alternatives to Two Populations of Seyfert 2 Galaxies*

Because the interpretation of two intrinsically different S2 types could potentially upset the currently popular UM paradigm, it is worthwhile to examine some of the alternatives and make certain that the two kinds of S2s are genuinely different. Besides being intrinsically weaker, possible reasons that the non-HBLR S2s may in fact be normal obscured S1s but are somehow able to escape detection include the following: (1) The S/N in some spectropolarimetric observations may simply be too low to detect weak HBLRs. This problem is exacerbated by the limited resolution (seeing) of ground-based telescopes, which must extract and detect precious scattered (polarized) photons against an overwhelming background of unpolarized starlight. (2) Placement and orientation of the spectroscopic slit in these observations may have missed a small or well-collimated scattering region. However, while some HBLRs could have escaped the detection limit of the survey, these possibilities alone cannot explain why the two S2 types lie in such separate regions of the diagnostic diagrams discussed above and have very distinct luminosity distributions (Figs. 10–12), with the HBLR S2s being generally more aligned with the S1 population.

Since the detectability of broad polarized Hα scales with the strength of the emission line, we can assess the detection limit of HBLRs in our survey by examining the distribution of the observed fluxes for some of the best indicators of AGN strength. Shown in Figure 14 is the plot of the observed extinction-corrected [O III] fluxes against the 25 μm mid-IR and 20 cm radio flux densities. A striking characteristic of this figure is that, contrary to the very significant differences seen in *luminosity* space (§ 2.2) for these three properties, there is no separation at all in flux space between the two S2 types. K-S tests show that these flux distributions are virtually the same between HBLR and non-HBLR S2s, with $p_{\rm null}$ ranging from 11% to 44%. Thus, a standard BLR is not any more likely to get detected in an HBLR S2 than a non-HBLR S2. It is also clear from Figure 14 that many HBLR detections reach to very low observed flux levels, below those of many non-HBLR S2s. For example, some of the HBLR detections are as much as an order of magnitude below the detection limit of $f_{\rm [O\,III]} = 10^{-12}$ ergs s^{-1} cm^{-2} estimated by Alexander (2001) for a 4 m class telescope. Thus, we conclude that there is no strong evidence for an observational bias against the detection of HBLRs in non-HBLR S2s and that their nondetections cannot all be simply due to the detection limit of the survey.

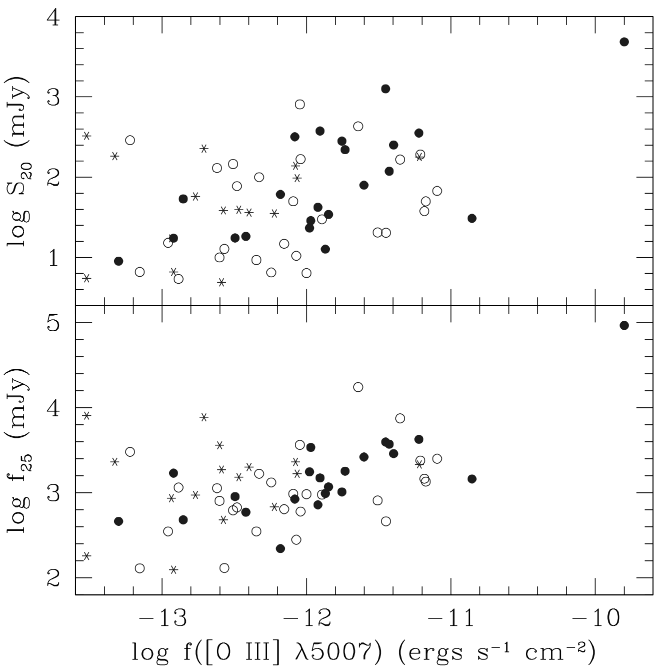

FIG. 14.—Extinction-corrected [O III] λ5007 fluxes vs. 25 μm mid-IR and 20 cm radio flux densities for the S2 and HLS galaxies in the CfA and 12 μm samples. These three properties have been shown to be good indicators of the AGN strength. Symbols are as in Fig. 1. The upper rightmost data point refers to NGC 1068. HBLR detection can reach to very low observed flux levels, below those of many non-HBLR S2s. In addition, the flux distributions are the same for the two S2 types, indicating that the non-detections of HBLRs cannot all simply be due to the detection limit of the survey. [*See the electronic edition of the Journal for a color version of this figure.*]

Paper I also addressed the question of whether the nondetection of HBLRs in non-HBLR S2 is due to the lack of an energetic AGN (and hence BLR) or to such exceptionally high obscuration that no signal from the buried AGN could be detected (i.e., $S_{20\,\mathrm{cm}}$ and f_{25}). Miller & Goodrich (1990) and later Heisler et al. (1997) suggested that the scattering may take place very close to the nucleus, in the inner "throat" of the torus, and that non-HBLR S2s are perhaps those with the torus axes tipped at larger inclinations, resulting in higher obscuration and greater obstruction of the scattering region. They would be expected to represent the Compton-thick AGNs, which show the highest X-ray absorption, with N_{H} in the range 10^{23}–10^{24} cm^{-2} and beyond. Aside from being in contrast with the observations that very extended scattering regions have been seen in many AGNs (e.g., Miller, Goodrich, & Mathews 1991; Tran et al. 1998, 2000; Cohen et al. 1999), this picture cannot be correct, since there are hints that very large inclinations have indeed been seen in HBLR AGNs (Tran et al. 1999). In addition, as found by Alexander (2001) and Paper I and discussed in the previous section, there is essentially no significant difference in the HX column density or other obscuration indicators, such as HX/[O III] and EW(Fe), between the HBLR and non-HBLR S2s, contrary to expectation if indeed HBLR S2s are preferentially viewed more pole-on. Another difficulty for the model is that mid-IR arguments indicate that there is *no* apparent difference in the optical depth between S1s and HBLR S2s, while that between the two S2 subtypes is unreasonably high (see § 3.2). Paper I also found that the Balmer decrements of the two S2 subtypes are similar (see Table 3), and Lumsden et al. (2001) have dismissed the notion of f_{25}/f_{60} being an indicator of viewing angle.

As emphasized in Paper I, the lack of HBLRs in the nondetected objects also cannot be easily attributed to a "contrast effect," in which the overwhelming contribution of starlight in the host galaxies may render any polarized signal difficult or impossible to detect. Starlight levels in HBLR S2s reaching ∼80%–90% are quite common (Tran 1995; Barth et al. 1999). Both HBLRs and non-HBLRs display similar levels of starlight domination, and the nondetection of an HBLR seems to be unrelated to it (Kay & Moran 1998; Tran et al. 1999), nor can it be simply attributed to a strong starburst coexisting with the AGN, "muddling" the picture. In this scenario, non-HBLRs may be cases where the starburst component is unusually strong, capable of contributing substantially to and "contaminating" the total energy output (e.g., Levenson, Weaver, & Heckman 2001b). González Delgado, Heckman, & Leitherer (2001) examined the question of whether starburst-dominated (i.e., "composites") and non-HBLR S2s are the same class of objects, using literature data available prior to our survey. They concluded that the answer appeared to be "no." With the present extended data set, we confirm that *not all* starburst-dominated S2s are non-HBLR S2s, and vice versa. Many starburst-dominated S2s have been found to be HBLRs, but by definition, *none* of the non-HBLRs are HBLRs. For example, there are 11 HBLR S2s detected to date in the sample of Cid Fernandes et al. (2001), with about half belonging to either the starburst/S2 composites or the normal S2s. So the relationship between starburst-dominated composites and non-HBLR S2s is not simple. Thus, the occurrence of an HBLR shows no strong preference for either the "composite" or "pure" systems. In addition, the average FIR luminosities of the two S2 types are indistinguishable, indicating no difference in their star-forming or starbursting properties.

Another possibility is that the nature of the obscuring medium may influence the detection of HBLRs. The non-HBLR S2s may belong to a class of AGNs in which the obscuring medium is not a torus at all but may take the form of a much more extended interstellar medium (MGT98) in the host galaxies. In this case, no strongly collimated "scattering cones" are expected, and thus no polarized broad lines are observed. In this model, the non-HBLR S2s would then represent largely those that show little or only modest X-ray absorption, with column densities expected to be in the range of Galactic values (i.e., $N_{\mathrm{H}} \sim 10^{20}$–$10^{21}$, or Compton thin). Again, this is contrary to their observed distributions of obscuration indicators discussed earlier. Alternatively, the torus opening may not be the same for all galaxies but is variable in size (e.g., Lawrence 1991), becoming larger with increasing AGN luminosity. In this scenario, the BLR and obscuring torus do exist in non-HBLR S2s with properties similar to those with a detectable HBLR (i.e., similar dust-to-gas ratio, composition, N_{H}, etc.), but the torus cone angles are considerably narrower, so narrow in fact that little or no ionizing radiation, and hence reflected light, could escape and be detected. One difficulty with this interpretation is that some of the most spectacular cases of ionization cones, which are neither narrow nor lacking in ionizing radiation, are found in non-HBLR S2s (e.g., Mrk 573 and NGC 5728; Wilson & Tsvetanov 1994; Schmitt & Kinney 1996).

If a hidden S1 exists in non-HBLR S2s, the simplest explanation for its nondetection may be that it is too weak to be detected and thus observationally "lacks" a BLR. The scattering region simply may not be able to exist in a Seyfert galaxy hosting an intrinsically weak S1 nucleus, or it may be too small to enable sufficient flux to be scattered (Lumsden & Alexander 2001), thus allowing the HBLR to be more easily detected. Again, the lack of an HBLR in sources with spectacular ionization cones is puzzling. Although none of the alternative models discussed seems to satisfactorily explain the differences and similarities presented in the previous section among the S1s and HBLR and non-HBLR S2s, this last interpretation is not inconsistent with the concept of two S2 populations: a more powerful (with an HBLR) nucleus would be expected to support a larger scattering region, while a weaker (non-HBLR) one may be able to sustain only a much smaller one or none at all. Similarly, the receding torus hypothesis can also accommodate the changing AGN strength with the varying opening of the torus that is central to the UM, potentially reconciling the two ideas.

3.2. *Large-Scale Properties of Seyfert Galaxies*

Given the seeming dichotomy of S2s suggested by our study, it would be of interest to ask if many of the differences found between S1s and S2s in the past could be explained by the fact that this dichotomy had not been taken into account. When data from previous studies, which assumed that *all* Seyfert galaxies of type 2 were equivalent, are reanalyzed in terms of the two S2 populations, with one being truly hidden S1s and the other real S2s, do the large-scale differences found in previous studies tend to disappear? This is the question that we would like to explore in this section.

There is already a hint that this is in fact the case when we examine the study of Schmitt et al. (2001), which selects Seyfert galaxies based on FIR flux and *warm* color. Unlike numerous earlier investigations, this study found no statistically significant differences between S1s and S2s in various properties, such as the host galaxy morphologies and frequency of companion galaxies. We argue that the differences reported in the past between S1s and S2s (e.g., MGT98; Dultzin-Hacyan et al. 1999) may have gone away in the Schmitt et al. study not, as has been claimed, because this sample is any more complete and based on more isotropic properties than previous surveys but *precisely* because of its selection effect: the sample preselects only *warm* Seyferts ($f_{25}/f_{60} > 0.27$), effectively discarding all weaker non-HBLR S2s. In other words, this sample really compares the normal S1s and their truly hidden counterparts: warm HBLR S2s. If this warm criterion were relaxed, the sample would undoubtedly contain a substantial number of weak or real S2s, LINERs, starbursts, and H II galaxies, all of which have a strong dust (FIR) component. Similar differences that were found in previous studies would likely be present again. A check on the statistics of HBLRs in the Schmitt et al. sample shows that about 70% of its S2s harbor HBLRs. The data are not complete (only ~40% of the S2s in the sample have currently been observed spectropolarimetrically), but this HBLR frequency is substantially higher than what was found by all previous surveys (Paper I; Moran et al. 2000; Lumsden et al. 2001). On the other hand, the sample of the de Robertis et al. (1998) study, in which a very significant difference is found between the mean environments of S1s and S2s, contains only one known HBLR S2 (NGC 4388). This study, therefore, compares properties mostly between S1s and non-HBLR S2s. These indications strongly argue for the concept that the two types of S2s are fundamentally different in nature. They also underscore the importance of separating out the truly hidden S1s (i.e., HBLR S2s) from the real S2s when comparing their properties to normal S1s.

To further illustrate that there may be no real difference between S1s and S2s when the HBLR and non-HBLR subtypes are properly accounted for, we take advantage of the marked increase in the currently known HBLR S2 population as a result of several recent spectropolarimetric surveys and reexamine some of the data of previous studies. We consider only HBLR S2s as the truly obscured S1 galaxies while excluding non-HBLR S2s from the comparison. When this is performed, the differences between S1s and S2s found by these studies tend to be insignificant. This provides one of the most compelling pieces of evidence to date for two S2 populations. We note that although some of our results may suffer from small-number statistics and/or incomplete samples, they are nevertheless useful as consistency checks of our hypothesis. Our reexamination includes observational evidence from the following studies:

1. Clavel et al. (2000) show that essentially all the S2s known to have HBLRs display mid-IR *Infrared Space Observatory* (*ISO*) spectra that look just like S1s, but those of S2s without HBLRs are indistinguishable from starburst galaxies. We find that the EWs of the 7.7 μm feature, usually attributed to polycyclic aromatic hydrocarbon (PAH), and the underlying local continuum luminosity show significant differences between HBLR and non-HBLR S2s. The Clavel et al. sample contains five HBLR S2s and 10 non-HBLR S2s that could be identified. The mean 7.7 μm PAH EWs are 0.921 ± 0.535 and 3.59 ± 1.72 μm for HBLRs and non-HBLRs, respectively. The corresponding means for the 7 μm monochromatic continuum luminosity are $\langle \log \nu L_{\nu,7} \rangle = 43.7 \pm 0.61$ and 42.6 ± 0.51 ergs s^{-1}. These distributions are different at the 0.9% and 2.8% significance level, respectively. On the other hand, their mean 7.7 μm PAH *luminosities* are indistinguishable at the 66% significance level (HBLR S2s: $\langle \log L_{7.7} \rangle = 42.7 \pm 0.74$ ergs s^{-1}; non-HBLR S2s: $\langle \log L_{7.7} \rangle = 42.2 \pm 0.65$ ergs s^{-1}).

Interestingly, the same quantities for S1s ($\langle \mathrm{EW}_{7.7} \rangle = 0.53 \pm 0.47$, $\langle \log \nu L_{\nu,7} \rangle = 43.73 \pm 0.85$, and $\langle \log L_{7.7} \rangle = 42.44 \pm 0.80$) display nearly identical behaviors compared to HBLR S2s but not to their non-HBLR counterparts: both S1s and HBLR S2s show much higher 7 μm continuum luminosity and lower 7.7 μm PAH EWs than non-HBLR S2s, while their 7.7 μm PAH luminosities are about the same. Since the PAH features are generally associated with intense starbursting regions, photodissociation regions, and galactic cirrus on a much larger scale unrelated to the nuclear activity (e.g., Laurent et al. 2000), these indications again suggest that the level of star formation is similar in these Seyfert galaxies; it is the active nuclear engine that is different. The differences and similarities found by Clavel et al. (2000) between the two main classes of S1s and S2s, therefore, can entirely be attributed to the presence of non-HBLR S2s in their sample. They interpreted these differences as being due to orientation effects similar to those proposed by Heisler et al. (1997). As argued in § 3.1, however, this model is untenable and thus cannot properly explain them. Specifically, Clavel et al. (2000) used the PAH EW as an indicator of the nuclear obscuration and derived an average difference in visual extinction of $A_V \approx 92$ mag between S1s and S2s. However, the same analysis would indicate a similar and unreasonably large difference in obscuration between the non-HBLR and HBLR S2s and virtually *no* difference between HBLR S2s and S1s, contrary to the UM. Rather than a reddening indicator, the PAH EW should more appropriately be viewed as a measure of the intrinsic nuclear *strength*. The mid-IR radiation therefore is a good measure of AGN activity.

2. From the three-component modeling of the *ISO* spectra of CfA Seyfert galaxies by Pérez García & Rodríguez Espinosa (2001), our examination shows that HBLR S2s have a strong warm dust component similar to that found in S1s, while non-HBLR S2s are characterized by dust that is generally cooler. The mean $F_{\rm warm}/F_{\rm IR}$ ratio for the four HBLR S2s in the Pérez García & Rodríguez Espinosa (2001) sample is 0.45 ± 0.13. This is comparable to the value of 0.42 for S1s but much higher than the 0.25 found for the non-HBLR S2s. Similarly, the mean $F_{\rm warm}/F_{20\,\rm cm}$ for HBLR S2s is 6.56 ± 0.34, comparable to 6.5 for S1s but higher than 6.1 for other S2s (Pérez García & Rodríguez Espinosa 2001).

From their observations, both Clavel et al. (2000) and Pérez García & Rodríguez Espinosa (2001) have indicated that the obscuring torus, if it exists, cannot be as optically thick as had been thought (e.g., Pier & Krolik 1992). As also suggested by other studies, even at near-IR to mid-IR wavelengths, the AGN radiation appears to be isotropic (Granato, Danese, & Franceschini 1997; Fadda et al. 1998) and may suffer from less extinction than commonly thought (Veilleux et al. 1997; Risaliti et al. 2000; Alonso-Herrero et al. 2001). This is confirmed by our finding that the distributions of L_{25} for S1s and S2s are very similar (Fig. 11 and Table 3). As also demonstrated in § 2.2, Paper I, and Lumsden & Alexander (2001), the well-known warmer f_{25}/f_{60} ratio in the HBLRs S2s compared to non-HBLR S2s is essentially a result of the former being intrinsically more luminous in mid-IR and suggests that even for highly obscured AGNs, the mid-IR signature of the powerful AGN can be seen. A lower optical thickness would also be consistent with evidence for lower optical/IR extinction than expected from HX column density, due perhaps to larger grain size in AGNs (e.g., Maiolino et al. 2001a, 2001b; Imanishi 2001) or the different spatial regions probed by the two wavelength regimes (Risaliti et al. 2000; Weingartner & Murray 2002). For this reason, the enormous A_V values often deduced from the HX $N_{\rm H}$, assuming standard dust/gas ratios and extinction curves, are highly suspect.

3. Based on a *Hubble Space Telescope* snapshot imaging survey of a large but heterogeneous sample of Seyfert galaxies, MGT98 found that the large-scale environments of Seyfert 1 and 2 galaxies are significantly dissimilar in terms of their dust morphologies. However, when the Seyfert sample of MGT98 is grouped separately into HBLR and non-HBLR S2s, the dust morphologies of the host galaxies of the former are statistically the same as S1s, which in turn are different compared to non-HBLR S2s. In the MGT98 sample, the fraction of non-HBLR S2s that show either dust lanes or absorption patches (designated D, DC, and DI in their paper) is 10/18, or 55%. The corresponding fraction for HBLR S2s is 3/11 (27%). Not only is this significantly lower than that for their non-HBLR cousins; it is essentially the same as for S1s (23%). Moreover, given that the dust incidence was found to be 39% for the total S2 population (MGT98), the above fractions are perfectly consistent with our finding that about half of them belong to each of the non-HBLR and HBLR subclasses [i.e., $(27 + 55)/2 = 41\%$].

4. As mentioned in this study, HBLR S2s have f_{25}/f_{60} and [O III]/Hβ ratios similar to S1s (see Fig. 1), while in non-HBLR S2s these ratios tend to be significantly smaller. Although the [O III]/Hβ ratio is on average smaller in non-HBLR S2, it is still well above the canonical value of 3 for Seyfert galaxies. Thus, these are truly bona fide Seyfert galaxies, not misclassified HLS objects, and the possibility that the latter may have " contaminated " the S2 sample has been eliminated. Rather, it is more likely that the line ratio can be explained by the fundamental difference in nuclear strength. This is further reinforced by the discovery that isotropic properties, such as L([O III]) and L_{25}, are found to be statistically the same between S1s and HBLR S2s, but they are significantly lower in non-HBLR S2s than in their HBLR counterparts (§ 2.2).

Schmitt (1998) also compared several emission-line ratios between S1s and S2s in his study. He found that the [O II]/[Ne III] and [O II]/[Ne V] ratios are statistically lower in S1s compared to S2s, indicating a higher excitation spectrum in the former. However, when a similar comparison is made between S1s and HBLR S2s only, we find that these differences are no longer statistically significant. The mean [O II]/[Ne III] ratio for the 12 HBLR S2s found in his sample is 2.6 ± 1.4. A K-S test against the S1 sample distribution (with a mean of 1.73 ± 0.8) yields $p_{\rm null} = 23\%$, confirming their similarity. For the [O II]/[Ne V] ratio, the number of available data for HBLR S2s is considerably smaller, rendering a statistical test less accurate, but it appears that there is also no significant difference between the mean of five HBLR S2s (2.3 ± 1.6) and that of S1s (1.54 ± 1.6). Thus, combined with the [O III]/Hβ property discussed earlier, these emission-line characteristics strongly suggest that the ionization of the narrow-line regions is very similar between S1s and HBLR S2s, while in non-HBLR S2s, it is statistically weaker. The puzzling line-ratio differences found by Schmitt (1998) between the two main Seyfert types need not invoke a special alignment of the torus axis with the host plane axis in S1s, as had been proposed. They can instead simply be explained by the existence of two populations of S2s, only one of which truly contains genuinely powerful hidden S1 nuclei capable of fully ionizing the extended NLR.

3.3. *Evolutionary Sequence of Seyfert Galaxies*

The possibility of two types of S2s has enormous implications for the nature of the Seyfert phenomenon and the UM of AGNs. For example, it shows that orientation alone does not fully account for the differences seen in all S1s and S2s. Moreover, it suggests that the fraction of HBLRs should increase with AGN power as determined, for example, by the radio luminosity of the AGN. This appears to be borne out by existing observations.

Let us assume that the fraction of HBLRs detected corresponds directly to the fraction of true AGNs in the population. By a " true " AGN, we mean energetic processes dominated by accretion power from a supermassive black hole *and* the existence of a detectable BLR. Cohen et al.

(1999) found that when combined with the results of Hill, Goodrich, & DePoy (1996), forming a complete, volume-limited sample of powerful narrow-line radio galaxies, the fraction of HBLRs detected is 6/9 (or 67%). In the radio-weak LINERS, the fraction of broad-line AGNs is comparable to or less than that found in the CfA S2 sample: of those HLS galaxies observed in the 12 μm sample, we find virtually none; Barth et al. (1999) found 3/14 (or 21%) in a random sample of LINERs. A systematic trend is noted in these surveys: the higher the radio power of the objects, the higher the fraction of AGNs found to possess HBLRs. This progression mirrors a similar trend already noted in ULIRGs: the higher the IR luminosity, the higher the fraction of true AGNs found in the sample (e.g., Veilleux et al. 1995). This provides support for the receding torus model of AGNs (Lawrence 1991), in which the torus opening increases with AGN luminosity. It also implies that low-luminosity AGNs, such as LINERs/Seyferts, may undergo an evolutionary process, already implicated in the higher luminosity ULIRGs and QSOs, in which nuclear activity is triggered, most likely through interactions with nearby neighbors, creating starbursts, (re)fueling the central massive black holes, and eventually forming AGN nuclei with BLRs (Osterbrock 1993; Heckman et al. 1995; Veilleux 2001). In this scenario, the real S2s and hidden S1s may simply be at different stages of this evolutionary path (see Hunt & Malkan 1999). A truly active nucleus with a BLR may arise once the activity level has reached above a threshold (e.g., Nicastro 2000), a notion also implied by the recent radio study of Ulvestad & Ho (2001), who suggested that a minimum level of activity is required for the Seyfert radio source to break out of its central engine.

That the non-HBLR S2s display emission-line ratios that qualify them as genuine Seyfert galaxies requires that there be some sort of hard nonstellar ionizing continuum. As shown in §§ 2.2 and 3.2, their spectra are generally characterized by lower excitation and lower luminosities. Any "contamination" by circumstellar starbursts may contribute to the lower ionization level observed in these objects, but not to their overall [O III], mid-IR, and radio luminosities. Thus, not all non-HBLRs are necessarily composites or have strong starburst components. As already discussed, many composites and starburst-dominated sources have also been found to possess HBLRs. The alternative is that the non-HBLRs are simply intrinsically weaker. Perhaps the central black hole is less massive or the accretion rate is smaller in these objects. The existence of a black hole mass–radio power relationship (Franceschini, Vercellone, & Fabian 1998; McLure et al. 1999; Gu, Cao, & Jiang 2001; Ho 2002; Wu & Han 2001) and the possible correlation between the incidence of broad-line objects with radio power strongly suggest that the black hole mass could play a crucial role in the AGN strength. Nicastro (2000) also suggested that there is an accretion rate threshold above which the BLR would appear. Thus, while it appears that much of the difference between S1s and S2s can be explained solely by orientation, it would be difficult for the same model to apply among the HBLR and non-HBLR S2s without invoking intrinsic physical differences. Again, it is reasonable that there is a component of evolution in this, that the non-HBLRs may represent dormant, "low-state" S2s whose activity has not yet been fully triggered. An evolutionary proposal to explain the starburst-Seyfert connection, which could be related to the development of the strength of the AGN engine and hence its BLR property, has also been envisioned by Storchi-Bergmann et al. (2001), Cid Fernandes et al. (2001), and Krongold, Dultzin-Hacyan, & Marziani (2002). Alternatively, real S2s may simply be those that have exhausted their fuel, and they may not be directly connected to S1s strictly through evolution.

4. CONCLUSIONS

We present evidence supporting the view that HBLR S2s are intrinsically more powerful than non-HBLR S2s. The positive detection of BLRs in HBLR S2s appears to be due largely to the intrinsic strength of the hidden AGN nucleus rather than the lower level of obscuration or the reduced dominance of the circumnuclear starburst. When the intrinsic difference between HBLR and non-HBLR S2s is taken into account, it is shown that the former, on average, share many similar large-scale characteristics with S1s, as would be expected if the UM is correct, while the latter do not. These results strongly suggest that not all S2s are intrinsically similar in nature, and HBLR S2s may be the only true counterparts to normal S1s. The incidence of HBLRs is found to have a tendency to increase with AGN strength, suggesting a temporal development in the torus opening angle, perhaps as the nucleus evolves from a state of relative quiescence to a full-scale AGN engine.

While our findings suggest two separate types of S2s and their evolutionary connections to S1s and each other, our study may suffer from selection effects inherent in samples not selected by isotropic properties (e.g., see Ho & Ulvestad 2001), such as those of the CfA and 12 μm samples. Small-number statistics and limited survey depth may also complicate some of the results. Future, deeper study of a more complete, unbiased sample of Seyfert galaxies will provide a firmer picture and further test the ideas proposed in this paper.

I thank M. H. Cohen, J. S. Miller, W. van Breugel, and H. Ford for their support while this research was being carried out through the years at Caltech, Lick Observatory, Lawrence Livermore National Laboratory, and The Johns Hopkins University. I am grateful to the staff at the Lick, Palomar, and Keck Observatories for their expert assistance during the observations and to G. Harper, P. Ogle, and R. Vermeulen for assistance with some of the observations and data reduction. I also wish to thank R. Antonucci, M. Malkan, T. Heckman, J. Krolik, and N. Levenson for useful discussions. Support from a NASA ACS grant and the Center for Astrophysical Sciences at JHU is gratefully acknowledged. The W. M. Keck Observatory is operated as a scientific partnership between the California Institute of Technology and the University of California, made possible by the generous financial support of the W. M. Keck Foundation. Work performed at LLNL is supported by the US Department of Energy under contract W7405-ENG-48. This research has made use of the CATS database (Verkhodanov et al. 1997) of the Special Astrophysical Observatory and the NASA/IPAC Extragalactic Database (NED), which is operated by the Jet Propulsion Laboratory, California Institute of Technology, under contract with NASA.

REFERENCES

Alexander, D. M. 2001, MNRAS, 320, L15
Alonso-Herrero, A., Quillen, A. C., Simpson, C., Efstathiou, A., & Ward, M. J. 2001, AJ, 121, 1369
Antonucci, R. R. J. 1984, ApJ, 278, 499
———. 1993, ARA&A, 31, 473
Antonucci, R. R. J., & Miller, J. S. 1985, ApJ, 297, 621
Barth, A. J., Filippenko, A. V., & Moran, E. C. 1999, ApJ, 525, 673
Bassani, L., et al. 1999, ApJS, 121, 473
Becker, R. H., White, R. L., & Helfand, D. J. 1995, ApJ, 450, 559
Bonatto, C. J., & Pastoriza, M. G. 1997, ApJ, 486, 132
Boroson, T. A., & Meyers, K. A. 1992, ApJ, 397, 442
Cid Fernandes, R., Heckman, T., Schmitt, H., González Delgado, R. M., & Storchi-Bergmann, T. 2001, ApJ, 558, 81
Cimatti, A., & di Serego Alighieri, S. 1995, MNRAS, 273, L7
Clavel, J., et al. 2000, A&A, 357, 839
Cohen, M. H., Ogle, P. M., Tran, H. D., Goodrich, R. W., & Miller, J. S. 1999, AJ, 118, 1963
Cohen, M. H., Ogle, P. M., Tran, H. D., Vermeulen, R. C., Miller, J. S., Goodrich, R. W., & Martel, A. R. 1995, ApJ, 448, L77
Cohen, R. D. 1983, ApJ, 273, 489
Collinge, M. J., & Brandt, W. N. 2000, MNRAS, 317, L35
Condon, J. J., Cotton, W. D., Greisen, E. W., Yin, Q. F., Perley, R. A., Taylor, G. B., & Broderick, J. J. 1998, AJ, 115, 1693
Condon, J. J., Huang, Z.-P., Yin, Q. F., & Thuan, T. X. 1991, ApJ, 378, 65
Coziol, R., Pena, M., Demers, S., & Torres-Peimbert, S. 1993, MNRAS, 261, 170
Coziol, R., Ribeiro, A. L. B., de Carvalho, R. R., & Capelato, H. V. 1998, ApJ, 493, 563
Cruz-Gonzalez, I., Carrasco, L., Serrano, A., Guichard, J., Dultzin-Hacyan, D., & Bisiacchi, G. F. 1994, ApJS, 94, 47
Dahari, O., & de Robertis, M. M. 1988, ApJS, 67, 249
de Grijp, M. H. K., Keel, W. C., Miley, G. K., Goudfrooij, P., & Lub, J. 1992, A&AS, 96, 389
de Robertis, M. M., & Osterbrock, D. E. 1986, ApJ, 301, 98
de Robertis, M. M., Yee, H. K. C., & Hayhoe, K. 1998, ApJ, 496, 93
Dopita, M. A., Heisler, C., Lumsden, S., & Bailey, J. 1998, ApJ, 498, 570
Duc, P.-A., Mirabel, I. F., & Maza, J. 1997, A&AS, 124, 533
Dultzin-Hacyan, D., Krongold, Y., Fuentes-Guridi, I., & Marziani, P. 1999, ApJ, 513, L111
Edelson, R. A., Malkan, M. A., & Rieke, G. H. 1987, ApJ, 321, 233
Fadda, D., Giuricin, G., Granato, G. L., & Vecchies, D. 1998, ApJ, 496, 117
Filippenko, A. V., & Halpern, J. P. 1984, ApJ, 285, 458
Franceschini, A., Vercellone, S., & Fabian, A. C. 1998, MNRAS, 297, 817
Gonçalves, A. C., Véron-Cetty, M.-P., & Véron, P. 1999, A&AS, 135, 437
González Delgado, R. M., Heckman, T., & Leitherer, C. 2001, ApJ, 546, 845
González Delgado, R. M., & Pérez, E. 1996, MNRAS, 280, 53
Goodrich, R. W. 1989, ApJ, 340, 190
Goodrich, R. W., & Miller, J. S. 1995, ApJ, 448, L73
Goodrich, R. W., Miller, J. S., Martel, A., Cohen, M., Tran, H. D., Ogle, P. M., & Vermeulen, R. C. 1996, ApJ, 456, L9
Granato, G. L., Danese, L., & Franceschini, A. 1997, ApJ, 486, 147
Gu, M., Cao, X., & Jiang, D. R. 2001, MNRAS, 327, 1111
Gu, Q.-S., Huang, J.-H., & Ji, L. 1998, Ap&SS, 260, 389
Heckman, T. M., et al. 1995, ApJ, 452, 549
Heisler, C. A., Lumsden, S. L., & Bailey, J. A. 1997, Nature, 385, 700
Heisler, C. A., Vader, J. P., & Frogel, J. A. 1989, AJ, 97, 986
Hill, G. J., Goodrich, R. W., & DePoy, D. L. 1996, ApJ, 462, 163
Hill, T. L., Heisler, C. A., Norris, R. P., Reynolds, J. E., & Hunstead, R. W. 2001, AJ, 121, 128
Hines, D. C., Schmidt, G. D., Smith, P. S., Cutri, R. M., & Low, F. J. 1995, ApJ, 450, L1
Hines, D. C., Schmidt, G. D., Wills, B. J., Smith, P. S., & Sowinski, L. G. 1999, ApJ, 512, 145
Hines, D. C., & Wills, B. J. 1995, ApJ, 448, L69
Ho, L. C. 2002, ApJ, 564, 120
Ho, L. C., Filippenko, A. V., & Sargent, W. L. W. 1997, ApJS, 112, 315
Ho, L. C., & Ulvestad, J. S. 2001, ApJS, 133, 77
Huchra, J., & Burg, R. 1992, ApJ, 393, 90
Hunt, L. K., & Malkan, M. A. 1999, ApJ, 516, 660
Imanishi, M. 2001, AJ, 121, 1927
Inglis, M., Hough, J. H., Axon, D. J., Bailey, J., & Ward, M. J. 1993, MNRAS, 263, 895
Iwasawa, K., Matt, G., Guainazzi, M., & Fabian, A. C. 2001, MNRAS, 326, 894
Iyomoto, N., Makishima, K., Fukazawa, Y., Tashiro, M., Ishisaki, Y., Nakai, N., & Taniguchi, Y. 1996, PASJ, 48, 231
Kay, L. E., & Moran, E. C. 1998, PASP, 110, 1003
Keel, W. C., de Grijp, M. H. K., Miley, G. K., & Zheng, W. 1994, A&A, 283, 791
Kirhakos, S. D., & Steiner, J. E. 1990, AJ, 99, 1722
Kollatschny, W., Fricke, K. J., Biermann, P., Huchtmeier, W., & Witzel, A. 1983, A&A, 119, 80
Krongold, Y., Dultzin-Hacyan, D., & Marziani, P. 2002, ApJ, 572, 169
Kruper, J., Urry, C., & Canizares, C. 1990, ApJS, 74, 347
Kukula, M. J., Pedlar, A., Baum, S. A., & O'Dea, C. P. 1995, MNRAS, 276, 1262
Laurent, O., Mirabel, I. F., Charmandaris, V., Gallais, P., Madden, S. C., Sauvage, M., Vigroux, L., & Cesarsky, C. 2000, A&A, 359, 887
Lawrence, A. 1991, MNRAS, 252, 586
Levenson, N. A., Cid Fernandes, R., Weaver, K. A., Heckman, T. M., & Storchi-Bergmann, T. 2001a, ApJ, 557, 54
Levenson, N. A., Weaver, K. A., & Heckman, T. M. 2001b, ApJ, 550, 230
Lipari, S., Bonatto, C., & Pastoriza, M. G. 1991, MNRAS, 253, 19
Lipari, S., Tsvetanov, Z., & Macchetto, F. 1993, ApJ, 405, 186
Lumsden, S. L., & Alexander, D. M. 2001, MNRAS, 328, 32L
Lumsden, S. L., Heisler, C. A., Bailey, J. A., Hough, J. H., & Young, S. 2001, MNRAS, 327, 459
Lutz, D., Maiolino, R., Moorwood, A. F. M., Netzer, H., Wagner, S. J., Sturm, E., & Genzel, R. 2003, A&A, in press
Maiolino, R., Marconi, A., & Oliva, E. 2001a, A&A, 365, 37
Maiolino, R., Marconi, A., Salvati, M., Risaliti, G., Severgnini, P., Oliva, E., La Franca, F., & Vanzi, L. 2001b, A&A, 365, 28
Maiolino, R., & Rieke, G. H. 1995, ApJ, 454, 95
Maiolino, R., Ruiz, M., Rieke, G. H., & Keller, L. D. 1995, ApJ, 446, 561
Malkan, M. A., Gorjian, V., & Tam, R. 1998, ApJS, 117, 25 (MGT98)
McLure, R. J., Dunlop, J. S., Kukula, M. J., Baum, S. A., O'Dea, C. P., & Hughes, D. H. 1999, MNRAS, 308, 377
Miller, J. S., & Antonucci, R. R. J. 1983, ApJ, 271, L7
Miller, J. S., & Goodrich, R. W. 1990, ApJ, 355, 456
Miller, J. S., Goodrich, R. W., & Mathews, W. G. 1991, ApJ, 378, 47
Miller, J. S., & Stone, R. P. S. 1993, Lick Obs. Tech. Rep. 66
Moran, E. C., Barth, A. J., Kay, L. E., & Filippenko, A. V. 2000, ApJ, 540, L73
Moran, E. C., Halpern, J. P., Bothun, G. D., & Becker, R. H. 1992, AJ, 104, 990
Moran, E. C., Kay, L. E., Davis, M., Filippenko, A. V., & Barth, A. J. 2001, ApJ, 556, L75
Murayama, T., Taniguchi, Y., & Iwasawa, K. 1998, AJ, 115, 460
Nicastro, F. 2000, ApJ, 530, L65
Ogle, P. M., Cohen, M. H., Miller, J. S., Tran, H. D., Fosbury, R. A. E., & Goodrich, R. W. 1997, ApJ, 482, L37
Oke, J. B., & Gunn, J. E. 1982, PASP, 94, 586
Oke, J. B., et al. 1995, PASP, 107, 375
Osterbrock, D. E. 1993, ApJ, 404, 551
Osterbrock, D. E., & de Robertis, M. M. 1985, PASP, 97, 1129
Osterbrock, D. E., & Martel, A. 1993, ApJ, 414, 552 (OM93)
Pappa, A., Georgantopoulos, I., & Stewart, G. C. 2000, MNRAS, 314, 589
Pappa, A., Georgantopoulos, I., Stewart, G. C., & Zezas, A. L. 2001, MNRAS, 326, 995
Pastoriza, M. G. 1979, ApJ, 234, 837
Pérez García, A. M., & Rodríguez Espinosa, J. M. 2001, ApJ, 557, 39
Pier, E. A., & Krolik, J. H. 1992, ApJ, 401, 99
Polletta, M., Bassani, L., Malaguti, G., Palumbo, G. G. C., & Caroli, E. 1996, ApJS, 106, 399
Risaliti, G., Elvis, M., & Nicastro, F. 2002, ApJ, 571, 234
Risaliti, G., Gilli, R., Maiolino, R., & Salvati, M. 2000, A&A, 357, 13
Risaliti, G., Maiolino, R., & Salvati, M. 1999, ApJ, 522, 157
Rodríguez-Ardila, A., Pastoriza, M. G., & Donzelli, C. J. 2000, ApJS, 126, 63
Roy, A. L., Norris, R. P., Kesteven, M. J., Troup, E. R., & Reynolds, J. E. 1994, ApJ, 432, 496
Ruiz, M., Efstathiou, A., Alexander, D. M., & Hough, J. 2001, MNRAS, 325, 995
Rush, B., Malkan, M. A., & Edelson, R. A. 1996, ApJ, 473, 130
Rush, B., Malkan, M. A., & Spinoglio, L. 1993, ApJS, 89, 1
Schmitt, H. R. 1998, ApJ, 506, 647
Schmitt, H. R., Antonucci, R. R. J., Ulvestad, J. S., Kinney, A. L., Clarke, C. J., & Pringle, J. E. 2001, ApJ, 555, 663
Schmitt, H. R., & Kinney, A. L. 1996, ApJ, 463, 498
Severgnini, P., Risaliti, G., Marconi, A., Maiolino, R., & Salvati, M. 2001, A&A, 368, 44
Slee, O. B., Sadler, E. M., Reynolds, J. E., & Ekers, R. D. 1994, MNRAS, 269, 928
Smith, D. A., Georgantopoulos, I., & Warwick, R. S. 2001, ApJ, 550, 635
Soifer, B. T., Boehmer, L., Neugebauer, G., & Sanders, D. B. 1989, AJ, 98, 766
Storchi-Bergmann, T., Baldwin, J. A., & Wilson, A. S. 1993, ApJ, 410, L11
Storchi-Bergmann, T., Bica, E., & Pastoriza, M. G. 1990, MNRAS, 245, 749
Storchi-Bergmann, T., González Delgado, R. M., Schmitt, H. R., Cid Fernandes, R., & Heckman, T. 2001, ApJ, 559, 147
Storchi-Bergmann, T., Kinney, A. L., & Challis, P. 1995, ApJS, 98, 103
Storchi-Bergmann, T., & Pastoriza, M. G. 1989, ApJ, 347, 195
Terashima, Y., Ho, L. C., & Ptak, A. F. 2000, ApJ, 539, 161
Thean, A., Pedlar, A., Kukula, M. J., Baum, S. A., & O'Dea, C. P. 2000, MNRAS, 314, 573
———. 2001, MNRAS, 325, 737
Tran, H. D. 1995, ApJ, 440, 565
———. 2001, ApJ, 554, L19 (Paper I)

Tran, H. D., Brotherton, M. S., Stanford, S. A., van Breugel, W., Dey, A., Stern, D., & Antonucci, R. 1999, ApJ, 516, 85
Tran, H. D., Cohen, M. H., & Goodrich, R. W. 1995, AJ, 110, 2597
Tran, H. D., Cohen, M. H., Ogle, P. M., Goodrich, R. W., & di Serego Alighieri, S. 1998, ApJ, 500, 660
Tran, H. D., Cohen, M. H., & Villar-Martin, M. 2000, AJ, 120, 562
Tran, H. D., Miller, J. S., & Kay, L. 1992a, ApJ, 397, 452
Tran, H. D., Osterbrock, D. E., & Martel, A. 1992b, AJ, 104, 2072
Ulvestad, J. S., & Ho, L. C. 2001, ApJ, 558, 561
Ulvestad, J. S., & Wilson, A. S. 1989, ApJ, 343, 659
Vaceli, M. S., Viegas, S. M., Gruenwald, R., & de Souza, R. E. 1997, AJ, 114, 1345
Veilleux, S. 2001, in Starburst Galaxies, Near and Far, ed. L. Tacconi & D. Lutz (Berlin: Springer), 88
Veilleux, S., Goodrich, R. W., & Hill, G. J. 1997, ApJ, 477, 631
Veilleux, S., Kim, D.-C., & Sanders, D. B. 1999, ApJ, 522, 113
Veilleux, S., Kim, D.-C., Sanders, D. B., Mazzarella, J. M., & Soifer, B. T. 1995, ApJS, 98, 171
Verkhodanov, O. V., Trushkin, S. A., Andernach, H., & Chernenkov, V. N. 1997, in ASP Conf. Ser. 125, Astronomical Data Analysis Software and Systems VI, ed. G. Hunt & H. E. Payne (San Francisco: ASP), 322
Véron-Cetty, M.-P., & Véron, P. 1986, A&AS, 66, 335
Weingartner, J. C., & Murray, N. 2002, ApJ, 580, 88
Whittle, M. 1992, ApJS, 79, 49
Wills, B. J., Wills, D., Evans, N. J., Natta, A., Thompson, K. L., Breger, M., & Sitko, M. L. 1992, ApJ, 400, 96
Wilson, A. S., & Tsvetanov, Z. I. 1994, AJ, 107, 1227
Winkler, H. 1992, MNRAS, 257, 677
Wu, X.-B., & Han, J. L. 2001, A&A, 380, 31
Young, S., Hough, J. H., Efstathiou, A., Wills, B. J., Axon, D. J., Bailey, J. A., & Ward, M. J. 1996a, MNRAS, 279, L72
Young, S., Hough, J. H., Efstathiou, A., Wills, B. J., Bailey, J. A., Ward, M. J., & Axon, D. J. 1996b, MNRAS, 281, 1206